# Fault interaction and stress triggering

# Types of interactions

| *Interaction type* | *Perturbation effects* | *Spatial scale* | *Temporal scale* |
|---|---|---|---|
| **Dynamic** | - Rupture propagation;<br>- Arrest | 1 – 60 Km | 1 – 20 s |
| **Static** | - Earthquake triggering;<br>- Off – faults aftershocks;<br>- Seismicity rate change | 1 – 60 Km<br>1 – 60 Km<br>1 – 100 Km | minutes – few years |
| **Post – seismic** | Long – term stress changes | 10 – 1000 Km | few years – centuries |

# Coulomb Failure Function

Following the Coulomb' s failure assumption we define a Coulomb Failure Stress as ( e. g. *Jaeger and Cook,1969* ):

$$CFS = \|T\| + \mu(\sigma_n + p_{fluid}) - C$$

where:

| | |
|---|---|
| $\|T\|$ | is the shear tration modulus, |
| $\mu$ | is the coefficient of friction, |
| $\sigma_n$ | is the normal stress ( positive in tension ), |
| $p_{fluid}$ | is the pore fluid pressure, |
| $C$ | is the cohesion. |

Assuming $\mu$ and $C$ constant over time, we have the Coulomb Failure Stress change:

$$\Delta CFS = \Delta\|T\| + \mu(\Delta\sigma_n + \Delta p_{fluid})$$

where it has been assumed an isotropic failure plane.

*ΔCFS* is used to evaluate if one earthquake brought another earthquake closer to, or farther from, failure:

*ΔCFS* > 0 ⇒ fault plane loaded ⇒ closer to failure

*ΔCFS* < 0 ⇒ fault plane relaxed ⇒ farther from failure

( Stress Shadow )

Neglecting the spatial dependence in tractions, are:

$\mathrm{T}(t) = \mathrm{T}(0) + \Delta\mathrm{T}(t)$ $\sigma_n(t) = \sigma_n(0) + \Delta\sigma_n(t)$ $p_{fluid}(t) = p_{fluid}(0) + \Delta p_{fluid}(t)$

Therefore we can write:

$$\Delta CFS(t) = \| \mathrm{T}(0) + \Delta\mathrm{T}(t) \| - \| \mathrm{T}(0) \| + \mu\left(\Delta\sigma_n(t) + \Delta p_{fluid}(t)\right)$$

$\Delta\|\mathrm{T}\|$ is the change in shear stress due to the first earthquake and it is resolved in the slip direction of the second earthquake;

$\Delta\sigma_n$ is the change in normal stress due to the first earthquake and it is resolved in the direction orthogonal to the fault plane of the second earthquake.

# Stress changes approaches ( after *Harris, 1998* )

| Method | Parameters Required | Successes | Problems | Authors |
|---|---|---|---|---|
| Static Coulomb failure stress (elastic) $\Delta CFS$ | mainshock static slip model, $\mu'$, and $\Delta\sigma$, $\Delta\tau$, $\dot{\tau}$, on known fault planes and known slip directions* | $\Delta CFS > 0$ explains locations of aftershocks that do occur, $\Delta CFS < 0$ predicts shadows (timing and locations); may give rupture extent | many $\Delta CFS > 0$ faults do not experience subsequent large earthquakes, so it is hard to use $\Delta CFS > 0$ as a predictive tool | *Smith and Van de Lindt* [1969], *Rybicki* [1973], *Yamashina* [1978], *Stein and Lisowski* [1983], *Simpson et al.* [1988], *Yoshioka and Hashimoto* [1989a, b], *Reasenberg and Simpson* [1992], etc. (see text for more authors); *Crider and Pollard* [this issue], *Hardebeck et al.* [this issue], *Harris and Simpson* [this issue], *Kagan and Jackson* [this issue], *Nalbant et al.* [this issue], *Nostro et al.* [this issue], *Taylor et al.* [this issue], and *Toda et al.* [this issue] |
| Dynamic Coulomb failure stress (elastic) $\Delta CFS(t)$ | mainshock dynamic fault slip model, $\mu'$, and $\Delta\sigma(t)$, $\Delta\tau(t)$ on known fault planes and known slip directions* | may predict rupture lengths, given fault geometry | does not explain long delays (more than tens of seconds) between subevents; needs more testing | *Harris et al.* [1991], *Harris and Day* [1993], *Hill et al.* [1993], *Gomberg and Bodin* [1994], *Spudich et al.* [1994, 1995], *Cotton and Coutant* [1997], etc. |
| Static rate and state | mainshock static slip model, $\Delta\sigma$, $\Delta\tau$, $\sigma$, $\tau$, $\dot{\tau}$, $A$, $B$, $D_c$, $H$, time of last event, recurrence interval (to determine slip speed) | seems to predict aftershock duration | needs more testing; rate-and-state parameters defined in the laboratory, but not known for the Earth | *Dieterich* [1994], *Dieterich and Kilgore* [1996], *Roy and Marone* [1996], *Gross and Bürgmann* [1998], *Gomberg et al.* [this issue], *Harris and Simpson* [this issue], and *Toda et al.* [this issue] |
| Dynamic rate and state | mainshock dynamic fault slip model, $\Delta\sigma(t)$, $\Delta\tau(t)$, $\sigma$, $\tau$, $\dot{\tau}$, $A$, $H$, time of last event, slip speed | may explain remote triggering | needs more testing; still need to define rate-and-state parameters in the Earth; inertial terms not yet included in models | *Dieterich* [1987] and *Gomberg et al.* [1997, this issue] |
| Static Coulomb failure stress (viscoelastic) | mainshock slip model, Maxwell relaxation time, relaxing layer thickness | may explain time delays between mainshock and subsequent events, also irregular recurrence intervals | needs more testing, also needs more geodetic data to confirm viscoelastic parameters | *Dmowska et al.* [1988], *Roth* [1988], *Ghosh et al.* [1992], *Ben-Zion et al.* [1993], *Taylor et al.* [1996], *Pollitz and Sacks* [1997], *Freed and Lin* [this issue] |
| Fluid flow | mainshock slip model, permeability tensor | may explain time delays between mainshock and subsequent events | may not be successful at predicting both the spatial and temporal aftershock pattern | *Li et al.* [1987], *Hudnut et al.* [1989], *Noir et al.* [1997], etc.; *Seeber et al.* [this issue] |

*If the aftershock fault planes are not known, then some authors assume optimally oriented faults; this requires knowledge of the background stress directions.

# 1 – D Spring – slider model

# Numerical Method: RK SS

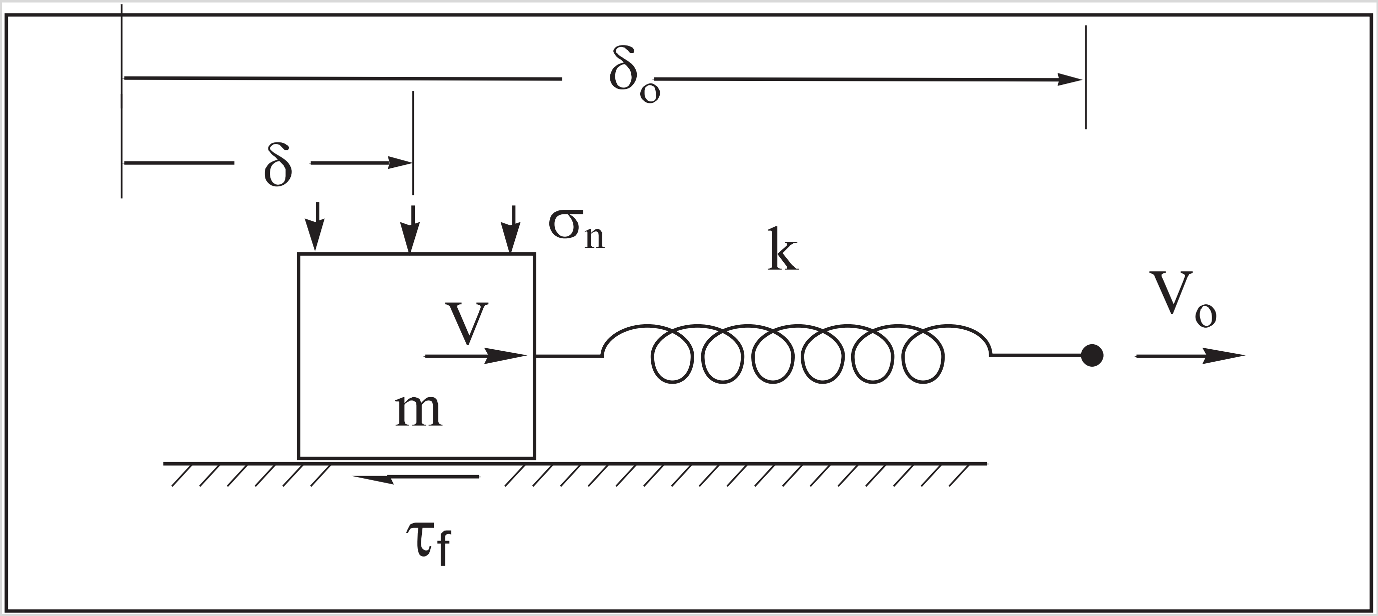


$$m\,\ddot{\delta} = k(\delta_o - \delta) - \tau_f + \Delta\tau, \quad \Delta\tau(t) \ \text{perturbazione}$$

$\tau_f$ = resistenza di attrito

**Reologia: attrito rate- and state-dependent**

$\theta$ ($\Phi$) = variable di stato della superficie, $V = \dot{\delta}$ velocità

**A - Ruina-Dieterich**

$$\tau_f = \tau_* + \ \theta + A \ln\left(\frac{V}{V_*}\right)$$

$$\frac{d\theta}{dt} = -\frac{V}{L}\,\theta + B \ln \frac{V}{V_*}$$

**B - Dieterich - Ruina**

$$\tau_f = \tau_* - A \ln\left(\frac{V_*}{V}\right) + B \ln\left(\frac{\Phi V_*}{L}\right)$$

$$\frac{d\Phi}{dt} = 1 - \frac{\Phi V}{L}$$

**Stato del sistema:** ($V(t)$, d $(t)$, $t_f(t)$)

*o condizioni mecc. faglia*

*appross. q. statica* ($V(t)$, $t_f(t)$)

*$V<V_C$=0.1 mm/s*

Inertia is negligible and the system passes through a sequence of equilibrium states

# Fault seismic cycle modeling

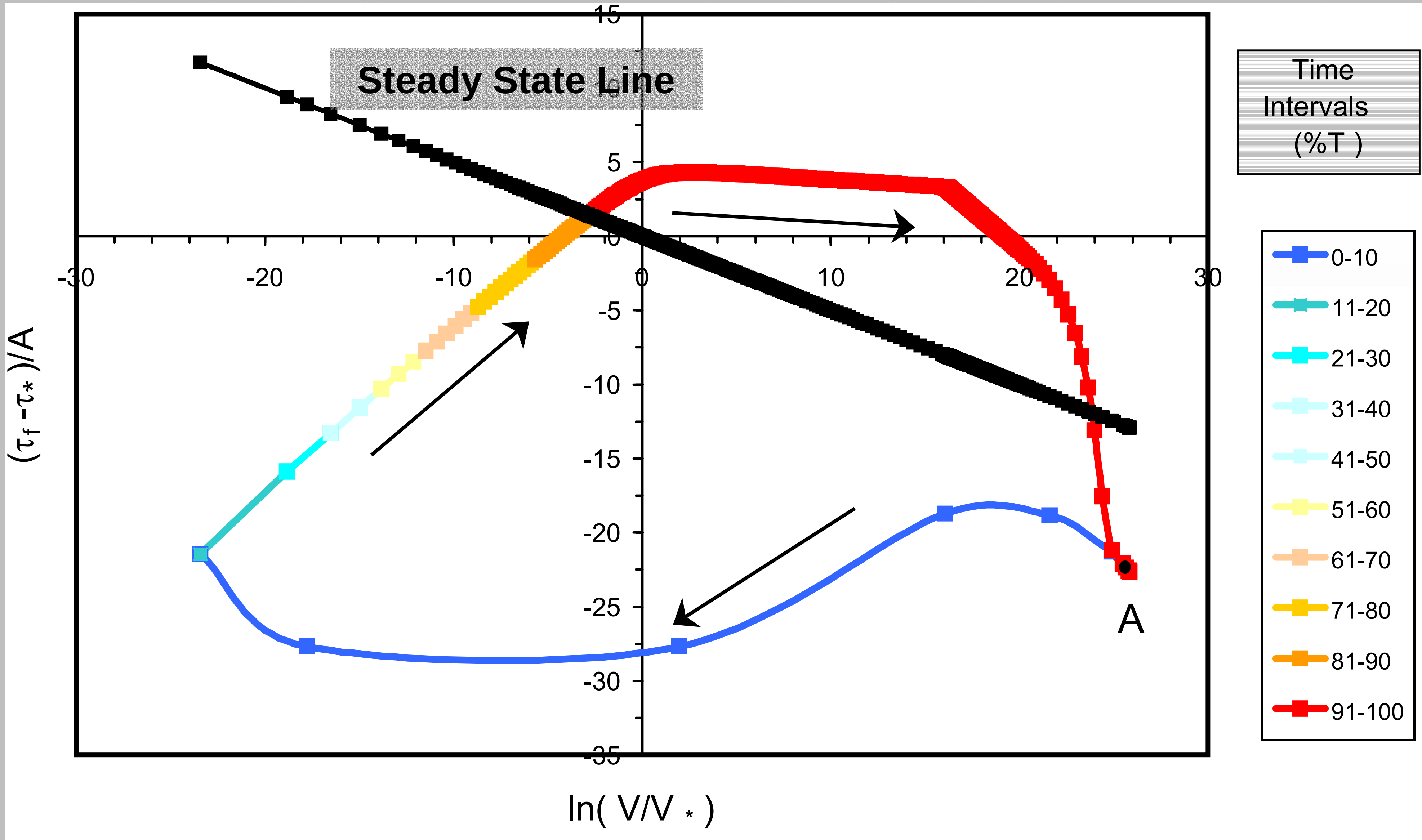

# Analytical stress perturbations

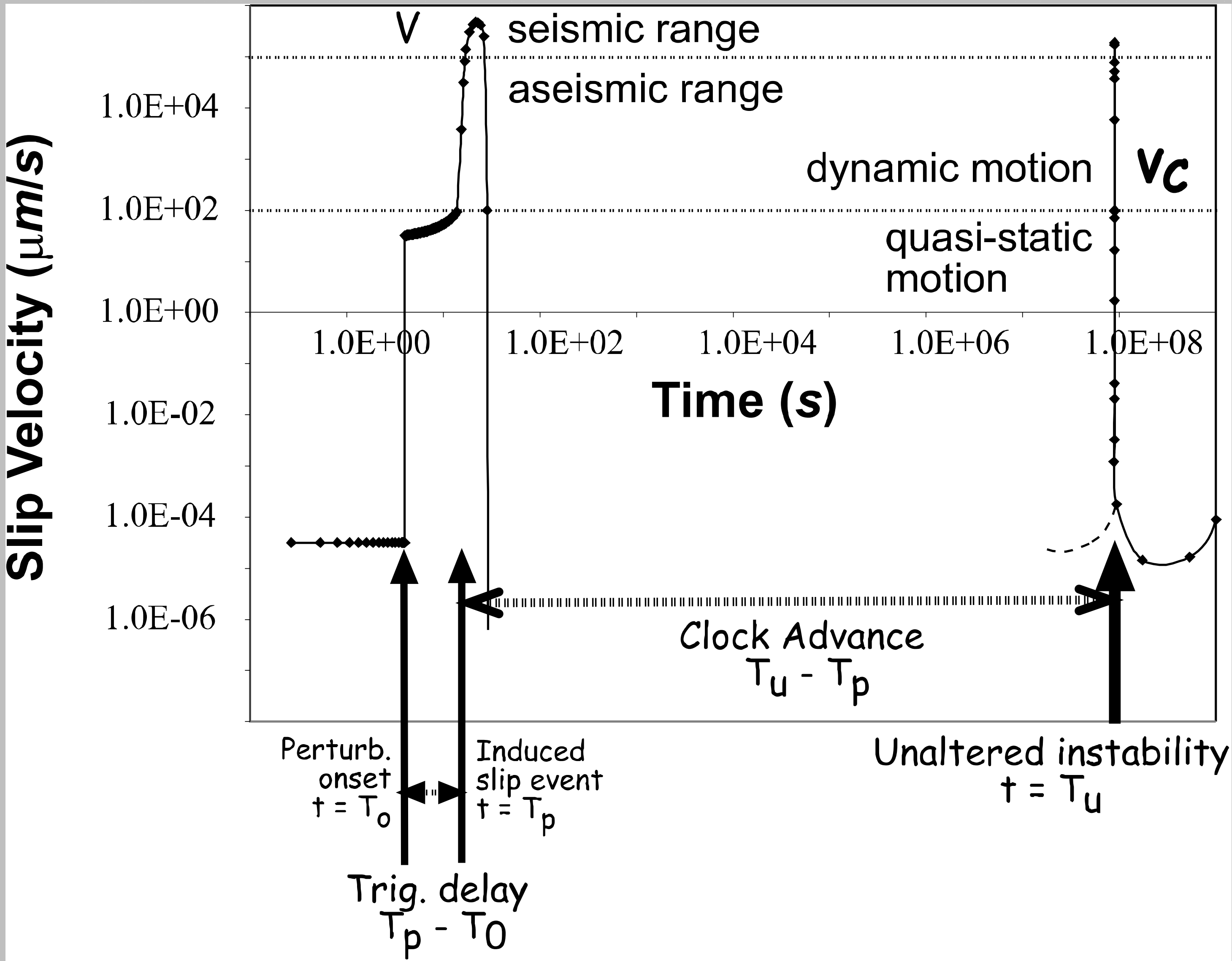

# Analytical stress perturbations
# The step and the pulse #1

## Step

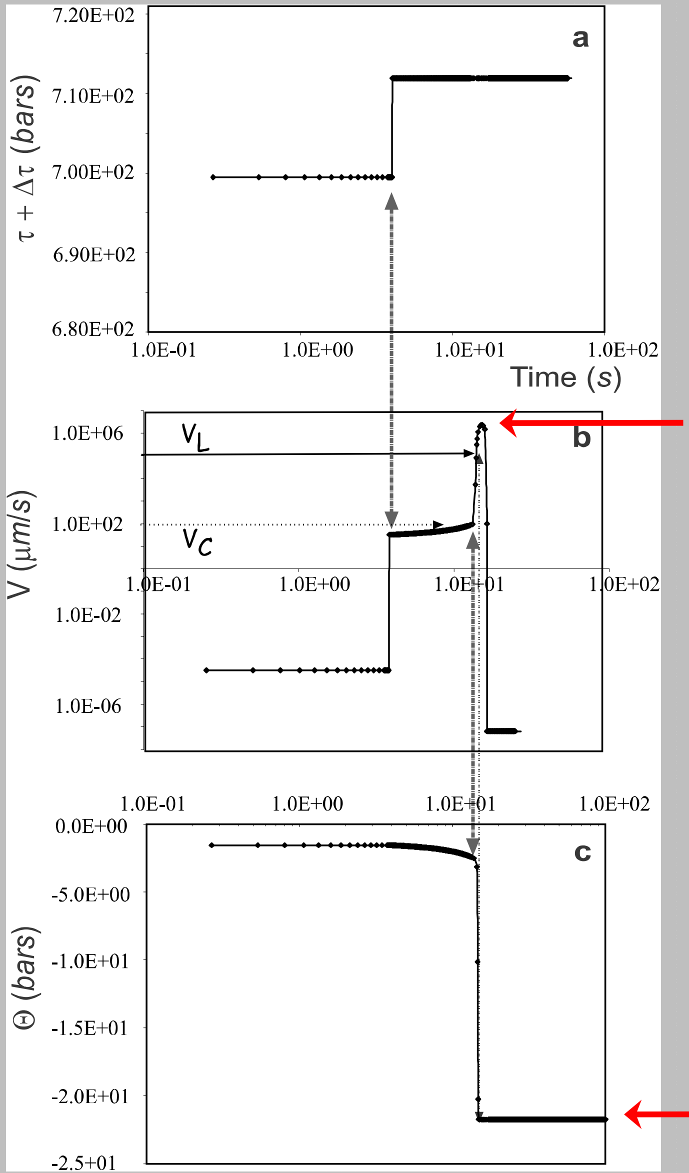


## Pulse

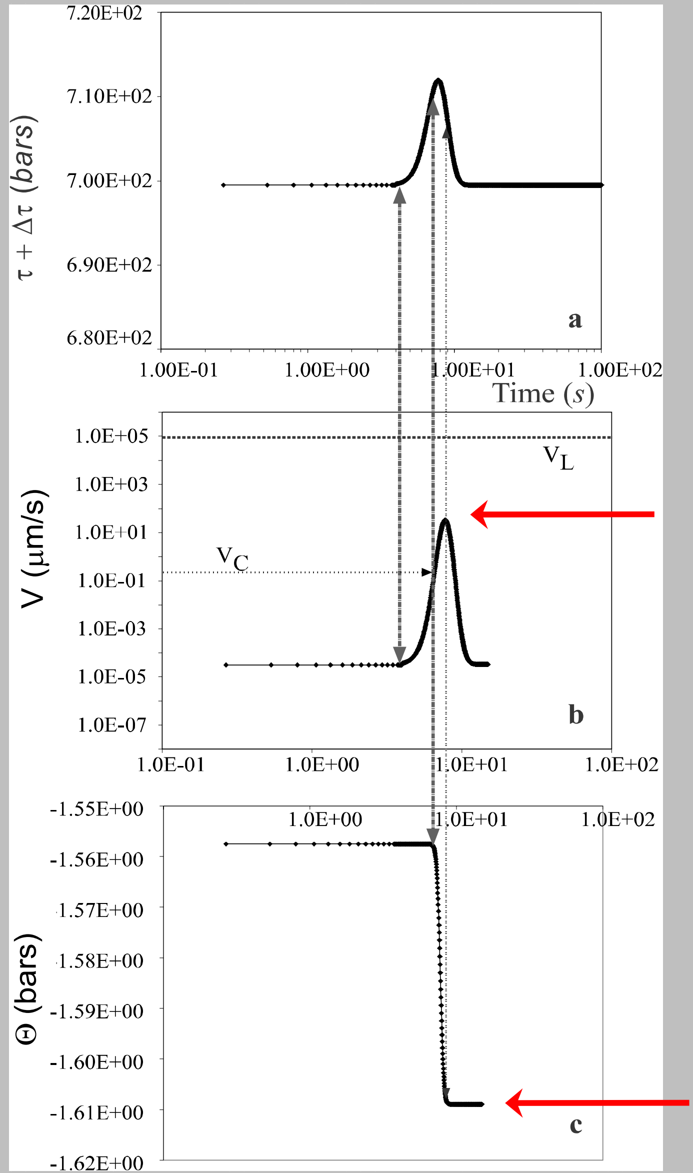

# Analytical stress perturbations
# The step and the pulse #2

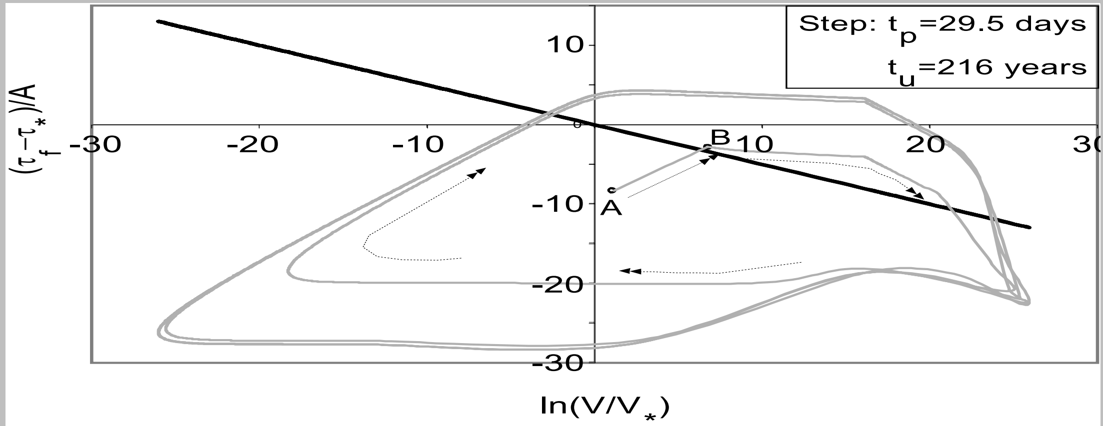


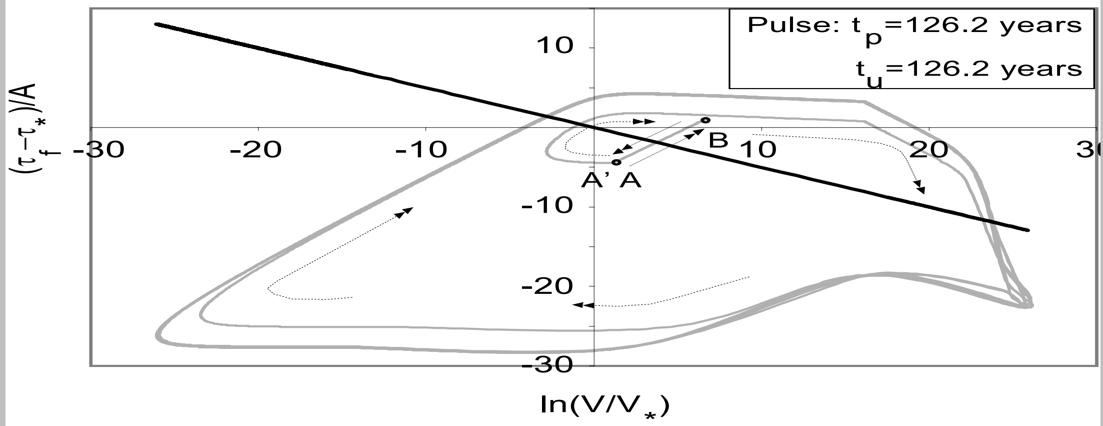

# Realistic stress perturbations
# Syntetic seismograms #1

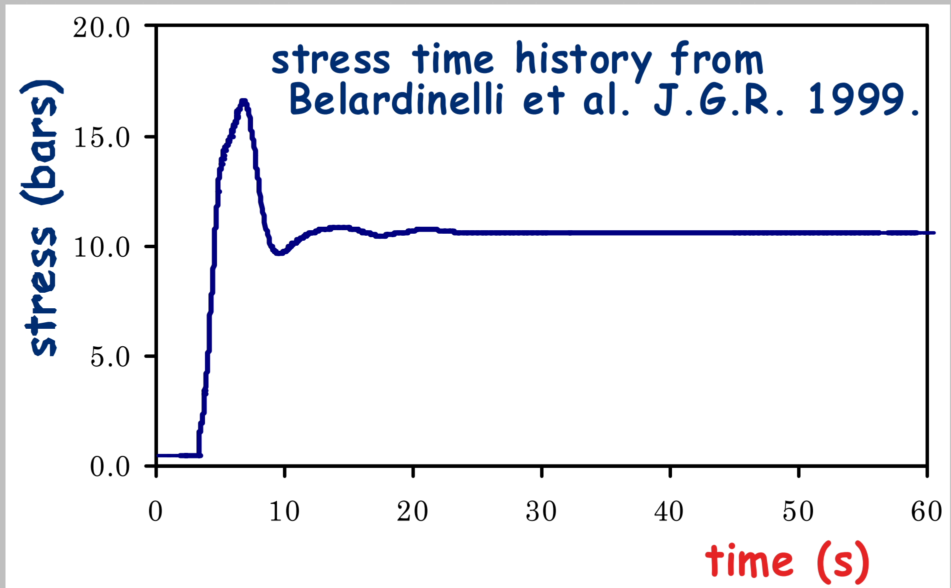


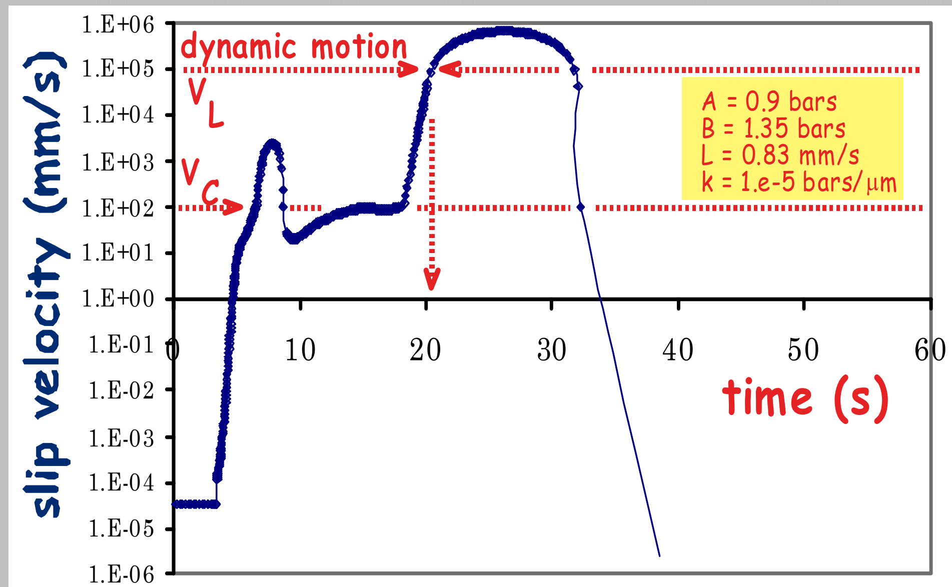

# Realistic stress perturbations
# Syntetic seismograms #2

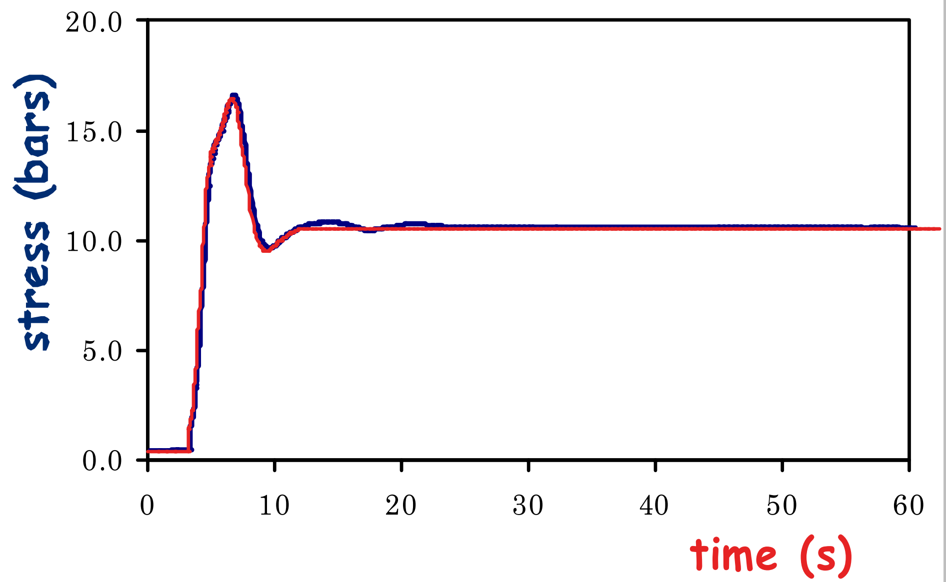


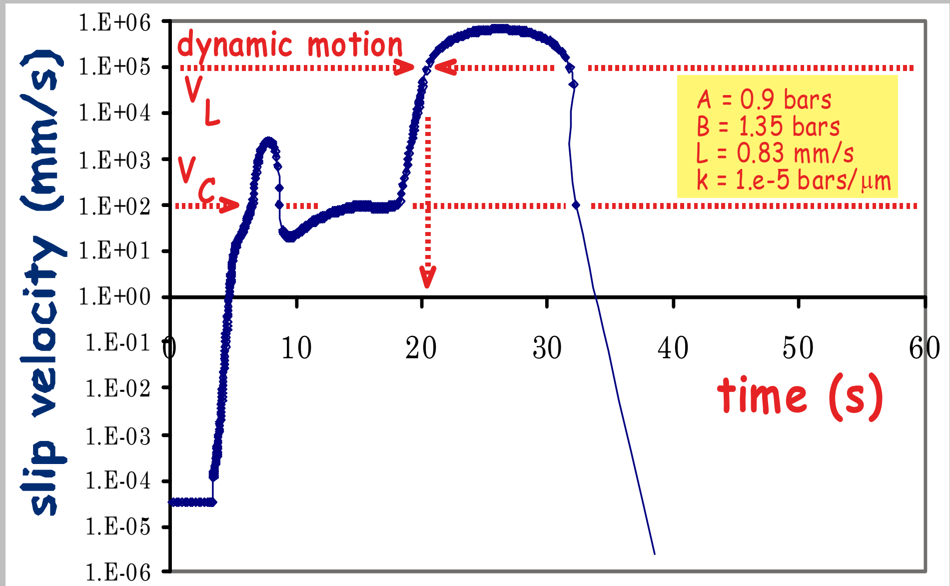

# Fault interaction by dynamic stress transfer: the case of the 2000 South Iceland seismic sequence

## Part I

# Motivations and Goals

- To evidence the eventual effect of the transient part of the coseismic stress changes due to the 17 June 2000, M 6.6 South Iceland earthquake;

- The debate on the triggering potential of transient stress changes is still open;

- The observational evidences are difficult and few.

# The choice of the events

- The largest events ( M ~ 5 ) occurring in the first five minutes
  - 8s, 26s, 30s, 130s, 226s
- in intermediate - far field
  - ~~8s~~, 26s, 30s, ~~130s~~, 226s
- that reasonably are not secondary aftershocks
  - 26s, 30s, ~~226s~~.

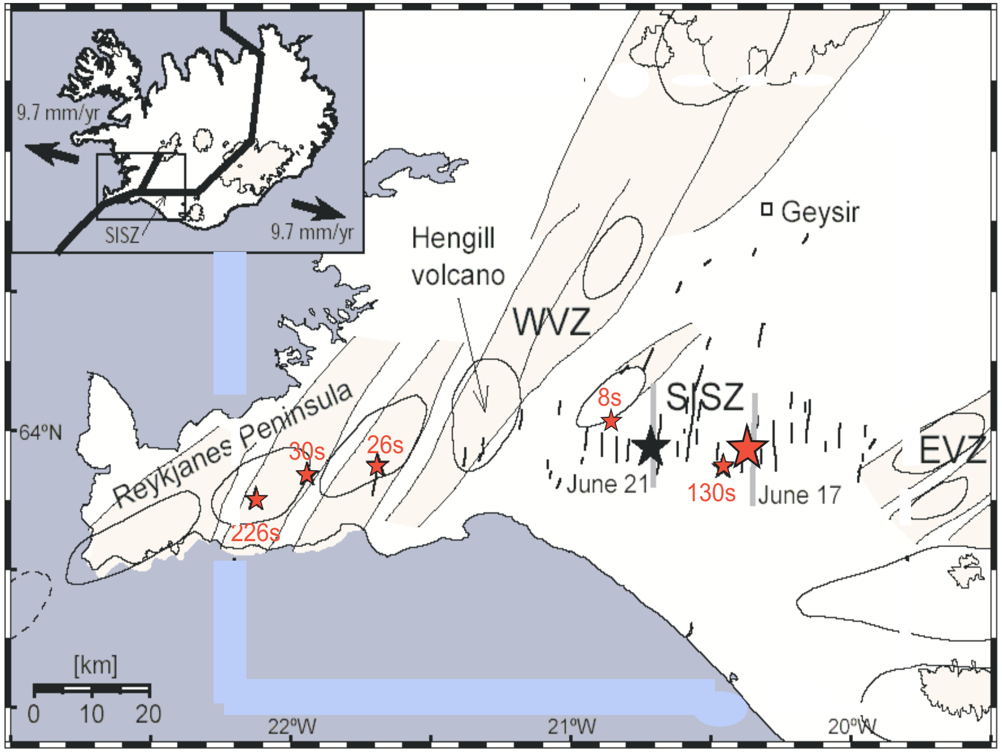

# The 26 s and 30 s events

- They were not detected teleseismically.
- **26 s** ( 64 km far )
  - –Not detected by DInSAR.
  - –Known fault.
- **30 s** ( 77 km far )
  - – Waveforms partially obscured by the first event ( mechanism uncertain )
  - – Detected by DInSAR and surface effects.
  - – August 2003: M 5 event on N-S fault with the same epicenter.

From SIL seismograms the 26 s and 30 s events occurred at the arrival ( later than the first ) of shear waves traveling at 2.5 km/s at their location.

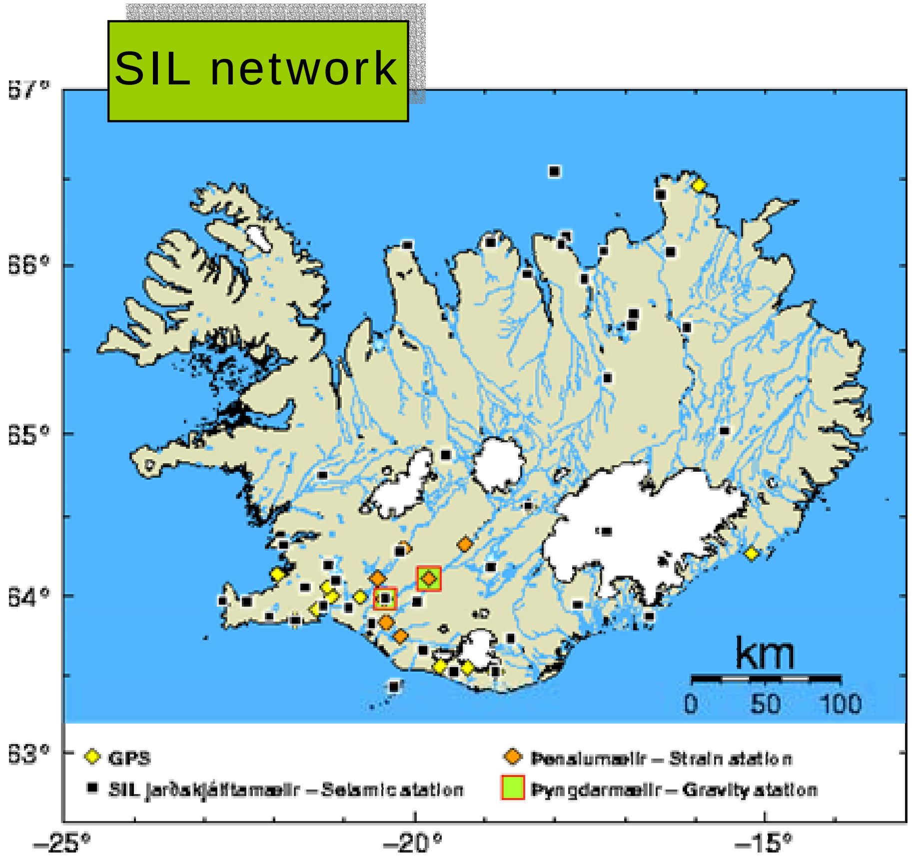


| Event | Origin time | Latitude (°) | Longitude (°) | Depth (km) | $M_L$ | $M_{Lw}$ |
|---|---|---|---|---|---|---|
| 26s | 154106.9 | 63.951 ±0.004 | -21.689 ±0.008 | 8.9 ±1.3 | 4.91 | 6 |
| 30s | 154111.254 | 63.937 ±0.003 | -21.94 ±0.01 | 3.8 ±1.3 | 4.68 | 5.9 |

# Parameters used to compute the dynamic stress

- Slip distribution from geodetic data ( Arnadottir et al. 2003 ). Right lateral strike slip fault, strike 7° E, dip 86°.
- Rupture history: bilateral Haskell model, rise time: 1-2 s, rupture velocity: 2.5 km /s.
- 2 crustal models with 4 layers:

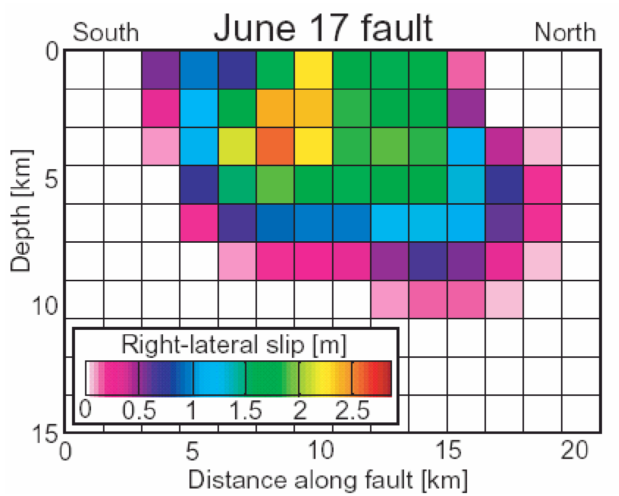


West of Hengill

| Depth (km) | $V_P$ (km/s) | $V_S$ (km/s) | Density (kg/m$^3$) |
|---|---|---|---|
| 0-3.1 | 3.3 | 1.85 | 2300 |
| 3.1-7.8 | 6.0 | 3.37 | 2900 |
| 7.8-17 | 6.85 | 3.88 | 3100 |
| >17 | 7.5 | 4.21 | 3300 |

East of Hengill

| Depth (km) | $V_P$ (km/s) | $V_S$ (km/s) | Density (kg/m$^3$) |
|---|---|---|---|
| 0-1.1 | 3.2 | 1.81 | 2300 |
| 1.1-3.1 | 4.5 | 2.54 | 2900 |
| 3.1-7.8 | 6.22 | 3.52 | 3100 |
| >7.8 | 6.75 | 3.8 | 3300 |

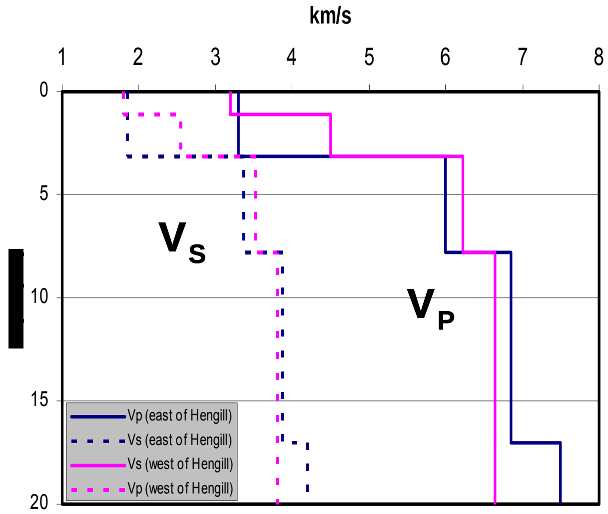

# Dynamic stresses at the two hypocenters

- Nord - Sud vertical right - lateral faults
- $\Delta CFF = \Delta\tau + \mu(1 - B)\Delta\sigma_n$, with $\mu$ = 0.75, $B$ = 0.47
- Rise time: 1.6 s

## 26 s aftershock

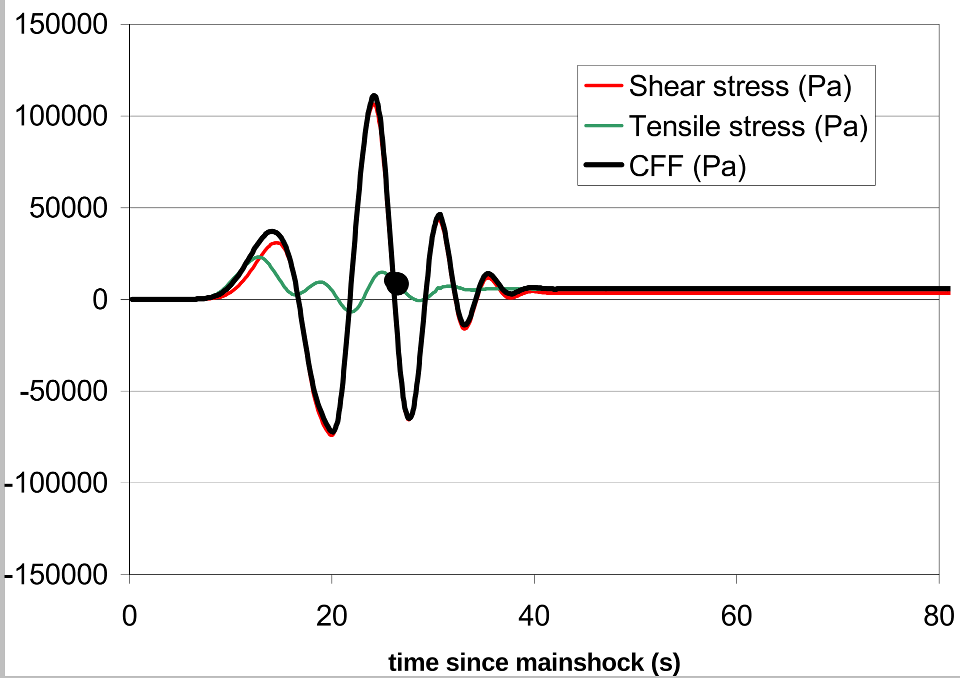


## 30 s aftershock

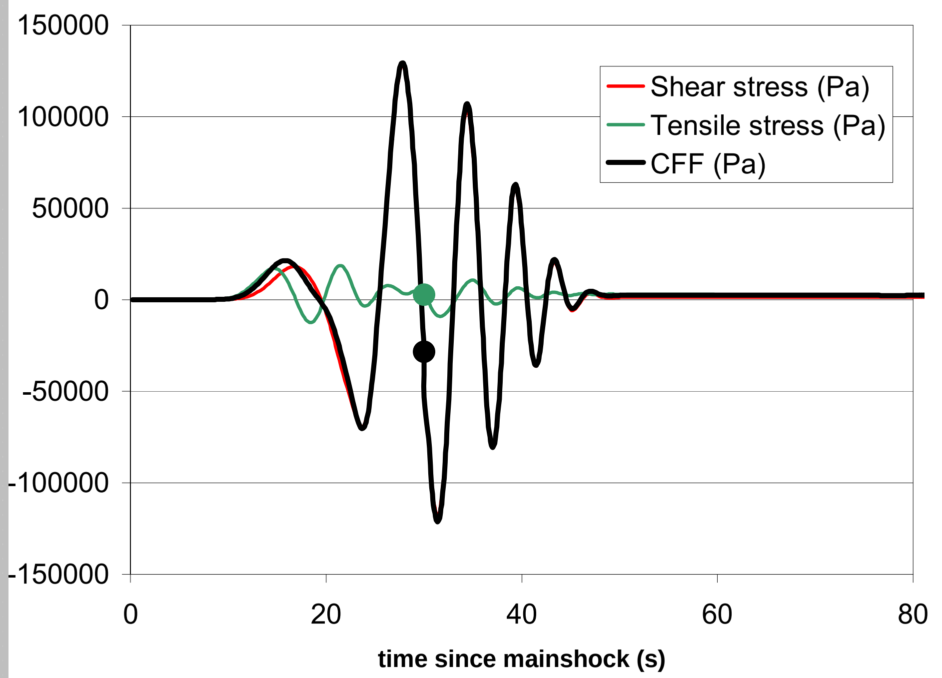

# *ΔCFF*(*t*) at the two hypocenters

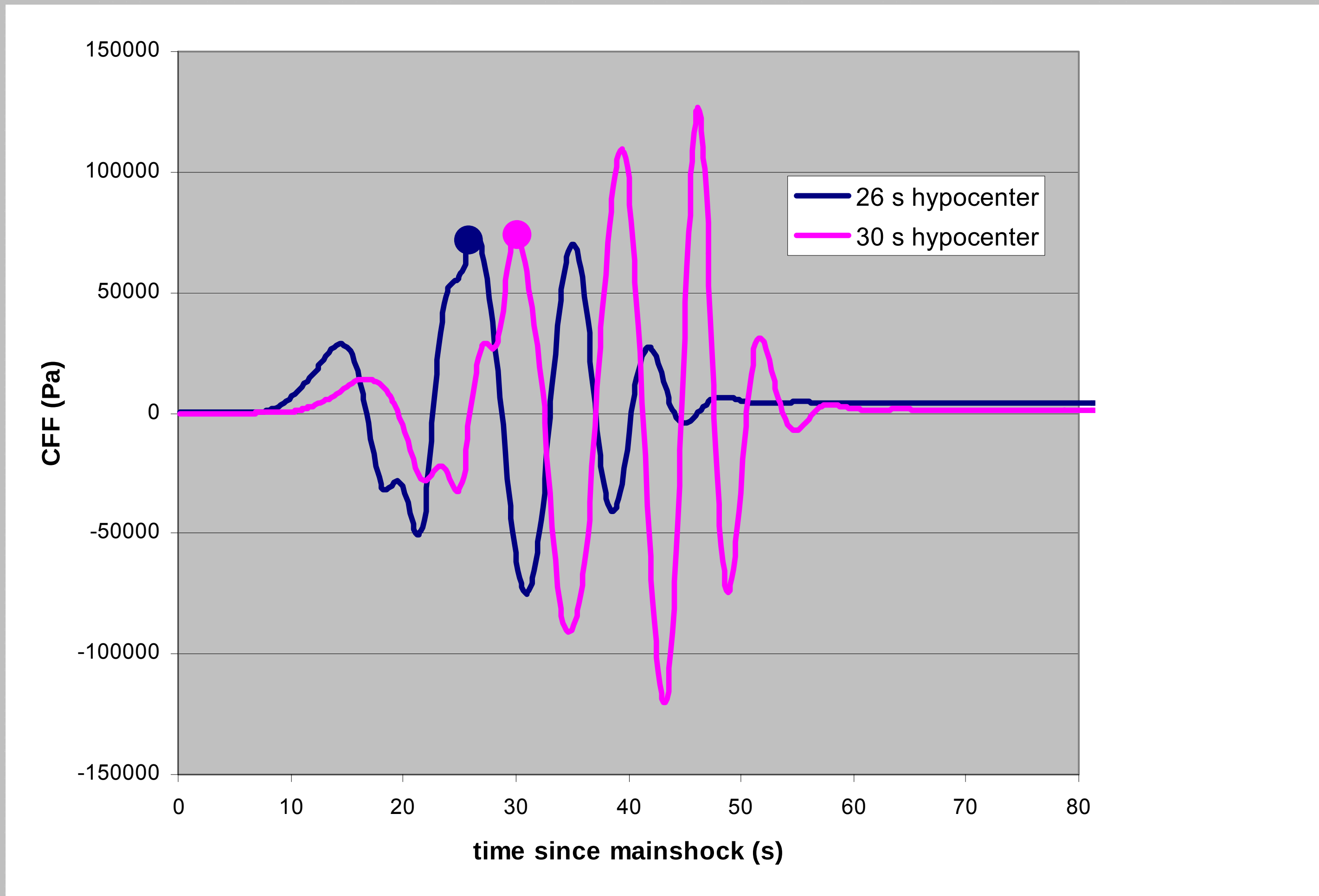


Time separation between the events and between stress peaks comparable.

# Snapshots of dynamic stress

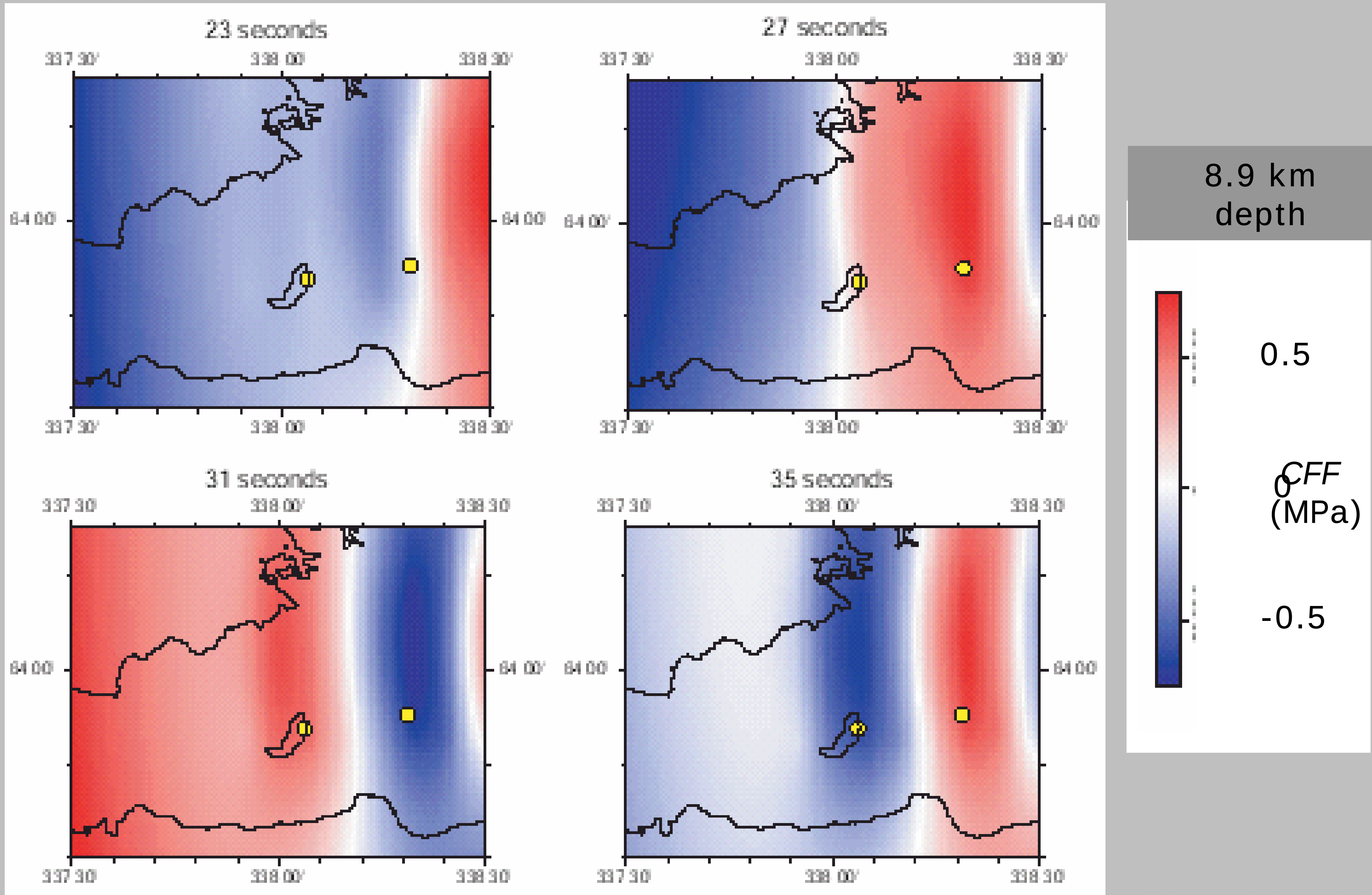

# Parameters sensitivity #1

- Stress at each hypocenter is affected by uncertain parameters such as the crustal model, rise time and the hypocentral depth.
- **Crustal model**

**26 s aftershock**

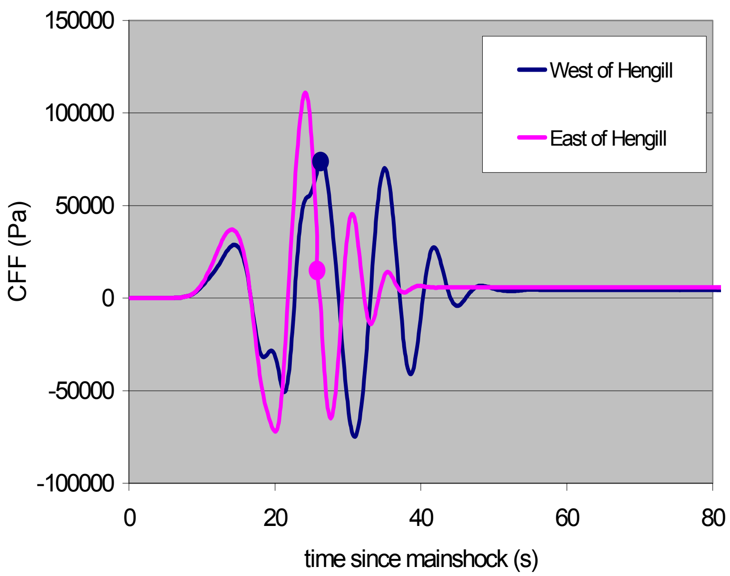


**30 s aftershock**

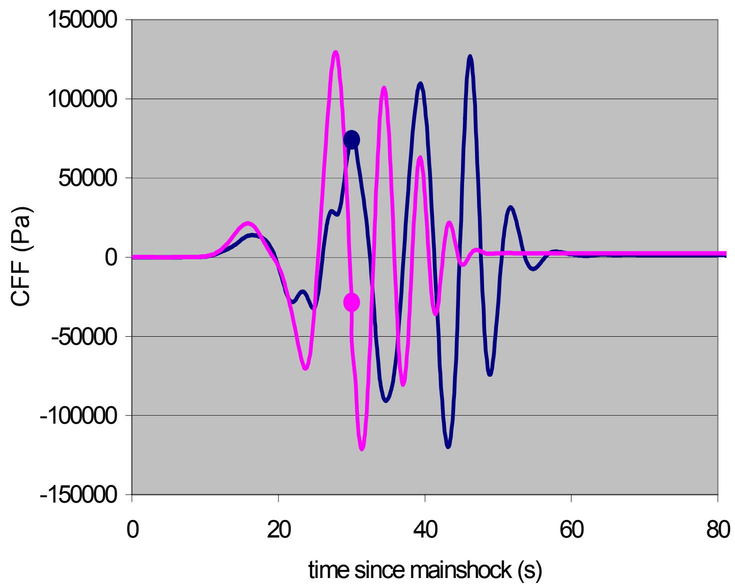


➢ The origin times ( from mainshock ) of the two events remain at, or follow closely the second CFF peak for ~ 1 - 2 s rise time.

# Parameters sensitivity #2

## Rise time

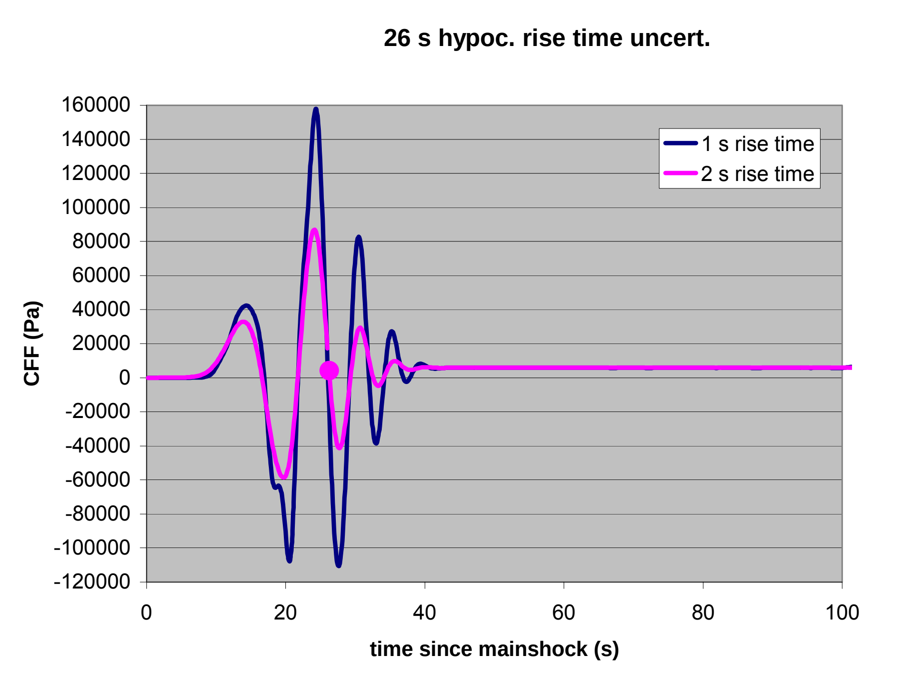


## Hypocentral depth

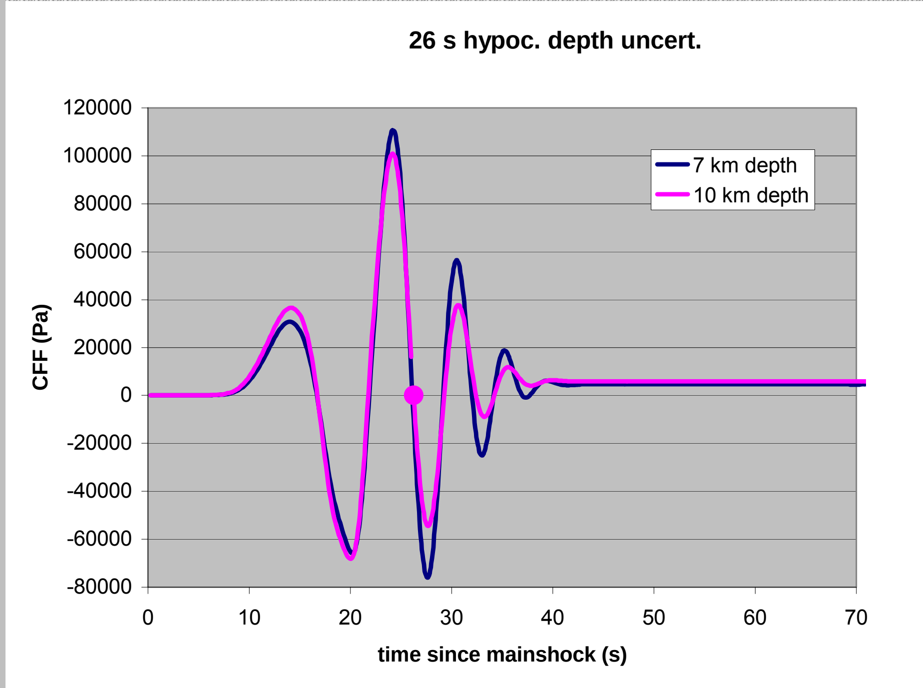


Uncertainties in stress amplitudes.

# The fault response

## Dieterich and Linker ( 1992 )

$$\tau = \left[ \mu_* + a \ln\left(\frac{v}{v_*}\right) + b \ln\left(\frac{\Psi v_*}{L}\right) \right] \sigma_n^{eff}(t)$$

$$\frac{\mathrm{d}}{\mathrm{dt}}\Psi = 1 - \frac{\Psi v}{L} - \alpha_{LD}\frac{\Psi \dot{\sigma}_n^{eff}}{b}$$

$$\alpha_{LD} = 0 \;\Rightarrow\; \sigma_n^{eff} = \sigma_n^{eff}(0)$$

- We study the fault response to the stress changes as evaluated at the two hypocenters with varying the parameters within their uncertaintes;
- We use a spring-slider model with rate- and state-dependent friction for variable effective normal stress $\sigma_n^{eff}$;
- The system is perturbed either in shear stress and normal stress ($\Delta\tau(t)$, $\Delta\sigma_n^{eff}(t)$);
- We investigate the possibility of instantaneous triggering (during the transient stress perturbation).

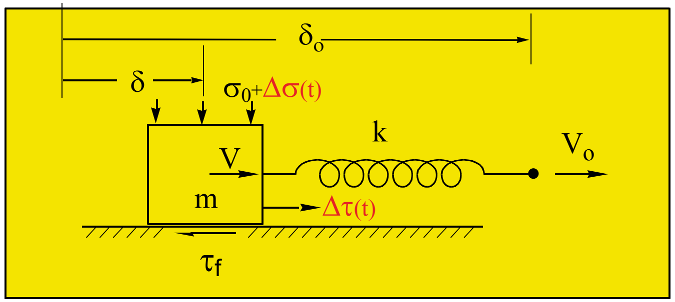


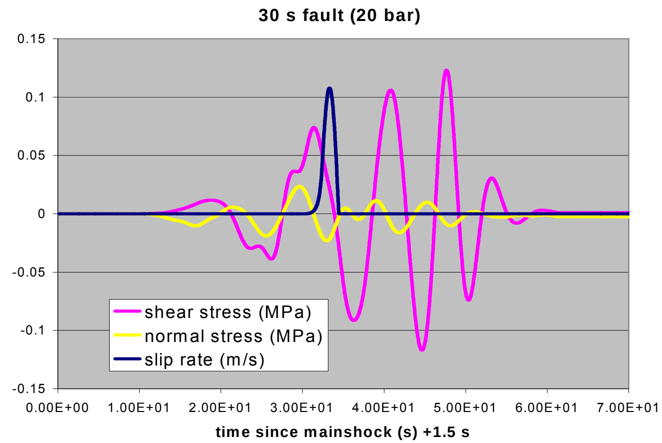

# The instantaneous trigger

1-D

- $h$ ~ 10 km linear fault dimension,
- standard values of rheological parameters ( $\mu_* = 0.7$, $L = 1$ mm, $b = 0.01$),
- $v_0 = 2$ cm/yr ( spreading rate in the SISZ ),
- fault in close to failure conditions ( 100% steady state ❾ unperturbed failure expected at less than 2 yr from June 17, 2000 )

➢ The fault tends to fail within 1 s after a peak in CFF, as evaluated at the two hypocenters

***if***

1. the initial effective normal stress $\sigma_0$ is enough low, so that the shear stress perturbation $\Delta\tau$ at that peak is much larger than $a(\sigma_0 + \Delta\sigma)$

2. and the direct effect of friction $a$ is enough low to keep fault unstable ( $k/k_{crit} < 1$ ) for low values of $\sigma_0$.

# Failure times of the perturbed faults

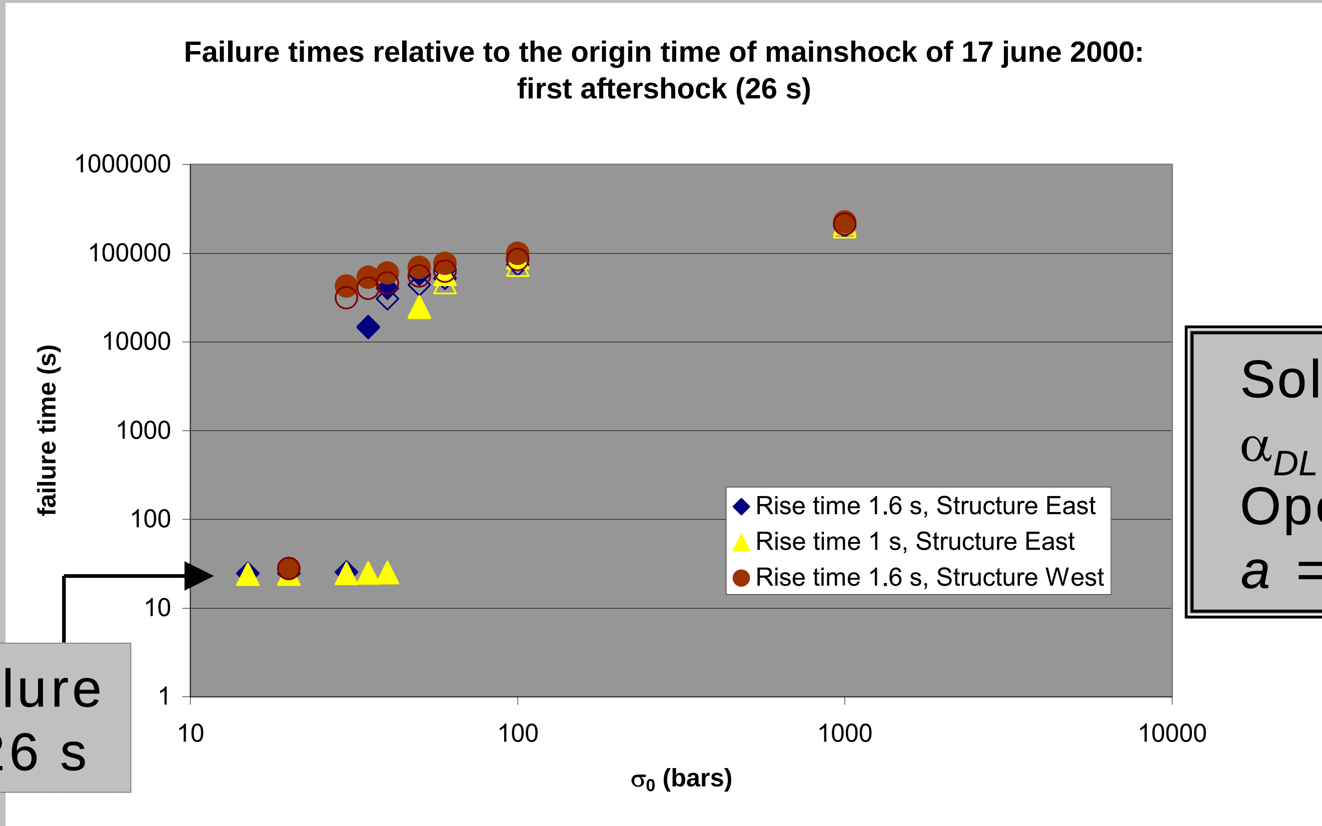


Mean failure time ≅ 26 s

Solid $\alpha_{DL}=0.56$
Open $\alpha_{DL}=0$
$a$ = 0.003

- For $a \leq 0.003$ and $\sigma_0 \cong 20$ bar, we obtained instantaneous trigger within 1 second after the second peak of CFF, as expected for the two aftershocks in the SISZ.
- For $a = 0.003$ and $\sigma_0 > \gamma$ 20 bar, $1 < \gamma < 10$ ( increasing with the amplitude of the second peak of $\Delta\tau$ ) the trigger is not instantaneous ( failure time > 4 hours ).

# Conclusions I

- ✓ The 26 and 30 s events occurred near one of the important geothermal areas of Iceland;
- ✓ They were neglibly affected by static stress changes;
- ✓ They followed closely a peak of positive CFF;
- ✓ These results favour the hypothesis of dynamic triggering;
- ✓ Dynamic models of fault responses can explain observations for low values of effective normal stress ( near lithostatic pore pressure ).

# Fault interaction by dynamic stress transfer: the case of the 2000 South Iceland seismic sequence

## Part II

The va ... up to
2.78 H ... spaced
1650 m ... 950 m,
6550 m

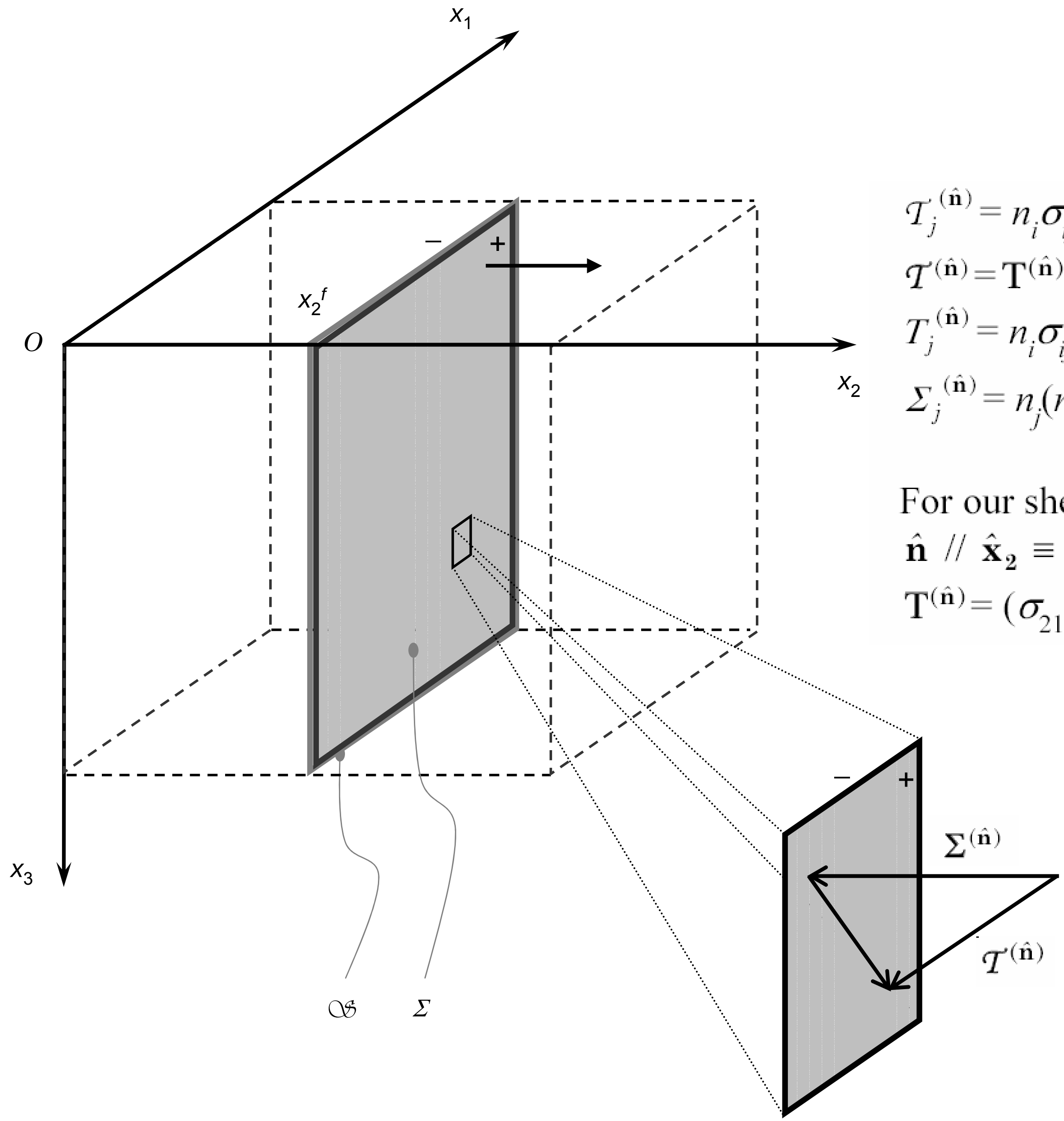


$$\mathcal{T}_j^{(\hat{\mathbf{n}})} = n_i \sigma_{ij}$$

$$\mathcal{T}^{(\hat{\mathbf{n}})} = \mathbf{T}^{(\hat{\mathbf{n}})} + \mathbf{\Sigma}^{(\hat{\mathbf{n}})}$$

$$T_j^{(\hat{\mathbf{n}})} = n_i \sigma_{ij} - n_j (n_i \sigma_{ik} n_k)$$

$$\Sigma_j^{(\hat{\mathbf{n}})} = n_j (n_i \sigma_{ik} n_k)$$

For our shear rupture:

$$\hat{\mathbf{n}} \ // \ \hat{\mathbf{x}}_2 \equiv (0,1,0)$$

$$\mathbf{T}^{(\hat{\mathbf{n}})} = (\sigma_{21}, 0, \sigma_{23})$$

The spatial sampling of the receiver grid is <u>not</u> sufficient to correctly resolve the dynamic processes occurring during the rupture nucleation and propagation (Bizzarri and Cocco, 2003; 2005), as well as the temporal discretization.

We develop an algorithm that employs a $\mathcal{C}^2$ cubic spline to interpolate $\Delta\sigma_{ij}$ in space and in time.

**Original values ( *t* = 26.37 s )**

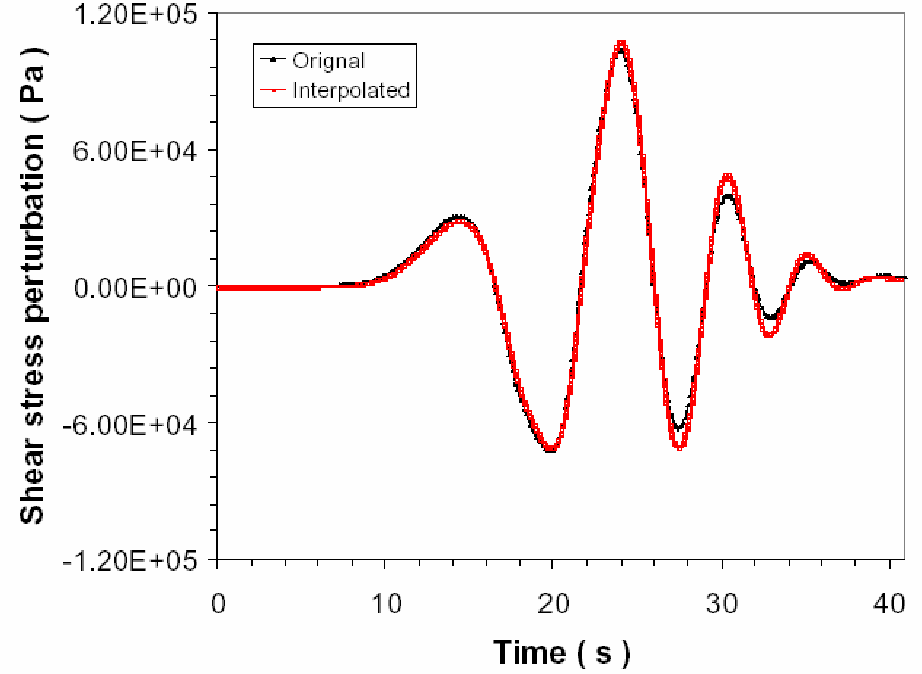


**Interpolated values ( *t* = 26.37 s )**

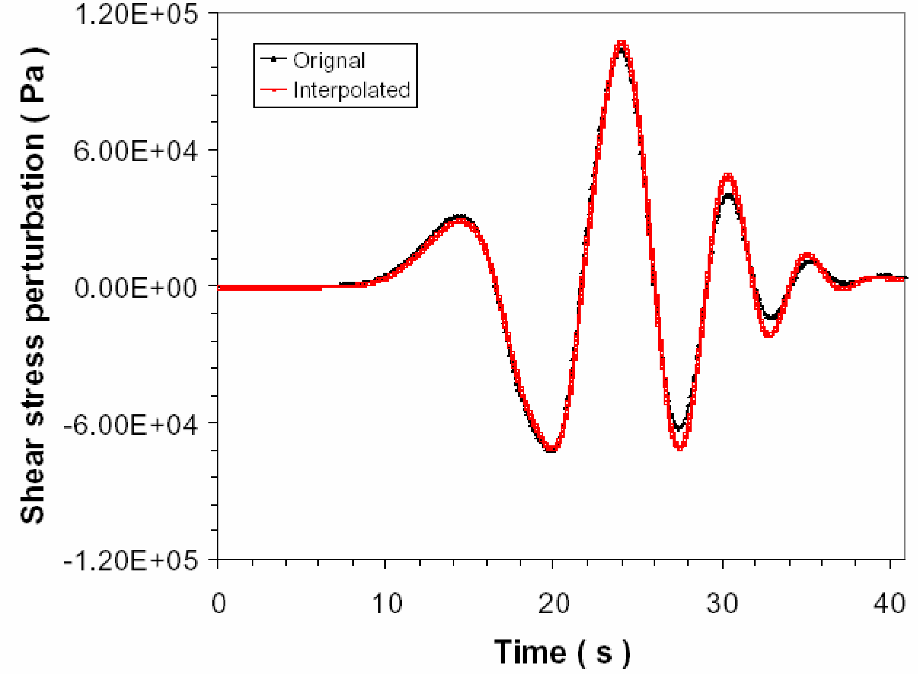

At time $t$, in each fault node, the dynamic load is: $\mathcal{L}_i = f_{ri} + T_{0i} + \Delta\sigma_{2i}$ ($i$ = 1 and 3).

$T_{0i}$ are the components of the initial traction ( $\mathrm{T}_{\mathbf{0}}(x_1, x_3) = \tau_0(x_1, x_3)(\cos(\varphi_0), 0, \sin(\varphi_0))$ )

$f_{ri}$ are the components of the load (namely the contribution of the restoring forces, $\mathbf{f}_{\mathbf{r}}$) exerted by the neighboring points:

$$f_{ri} = (M^- f_i^+ - M^+ f_i^-)/(M^+ + M^-),$$

where $M^+$ and $M^-$ are the masses of the "+" and "–" half split–node of the fault plane $\Sigma$ and $\mathbf{f}^+$ is the force acting on partial node "+" caused by deformation of neighbouring elements located in the "–" side of $S$ (and viceversa for $\mathbf{f}^-$).

$\{\Delta\sigma_{2i}\}$ are coupled to the components of the fault friction $T_i$ via

$$\frac{\mathrm{d}^2}{\mathrm{d}t^2} u_1 = \alpha[\mathcal{L}_1 - T_1]$$
$$\frac{\mathrm{d}^2}{\mathrm{d}t^2} u_3 = \alpha[\mathcal{L}_3 - T_3]$$

where $\alpha \equiv \mathcal{A}\,((1/M^+) + (1/M^-))$, $\mathcal{A} = \Delta x_1 \Delta x_3$. $T_i$ express on the governing law.

# Observational constraints

1) Perturbed rupture time $t_r = 25.9 \pm 0.1$ s

2) Hypocenter (63.951 ± 0.004 °N, 21.689 ± 0.008 °W, 8.9 ± 1.3 Km) ↔ on fault coordinates of (16500 ± 450, 8900 ± 1300) m (Antonioli et al., 2005)

3) From the aftershocks distribution shown in Hjaltadottir and Vogfjord (2005) we consider the seismic part of the fault (A) limited in latitude between 63.890 °N and 63.951 °N (in the case of Nord–South fault this corresponds to [9700, 16500] m in strike direction) and limited in depth between 5400 m and 7400 m

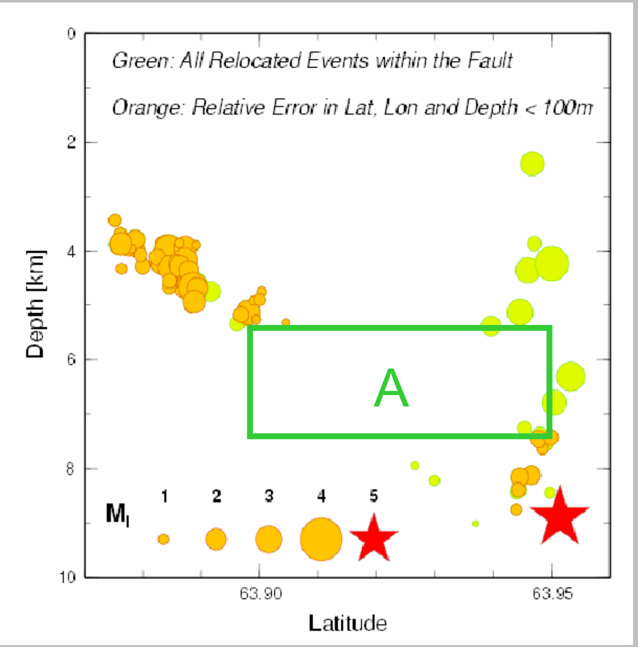


Upper bound estimates:

$M_0 = 1.23 \times 10^{15} A^{3/2} = 6.15 \times 10^{16}$ Nm;

Av. fault slip: $\langle u \rangle_A = M_0/(\rho v_S^2 A) = 0.12$ m;

Av. stress drop: $\langle \Delta\tau \rangle_A = 2M_0/(\pi W_A L_A) = 1.44$ MPa

4) $M_w \geq 5$ (Arnadottir et al., 2006; Vogfiord, 2003) $\Rightarrow M_0 \cong 3.2 \times 10^{16}$ Nm

# Results with DR law – homogeneous

## Dieterich – Ruina governing law

$$\tau = \mu(v,\Psi)\sigma_n^{eff} = \left[\mu_* + a\ \ln\left(\frac{v}{v_*}\right) + b\ \ln\left(\frac{\Psi v_*}{L}\right)\right]\sigma_n^{eff}$$

$$\frac{d}{dt}\Psi = 1 - \frac{\Psi v}{L}$$

Can be neglected (see Antonioli et al., 2005)

## Perturbed rupture times

$v(x_1,x_3,t) \geq v_l \Rightarrow t_p(x_1,x_3) = t$

$v_l$ = 0.1 m/s, in agreement with Belardinelli at al. (2003); Antonioli et al. (2005); Rubin and Ampuero (2005); Ziv and Cochard (2006)

## $\sigma_n^{eff}$ = 2.5 MPa everywhere; acting only $\Delta\sigma_{21}$

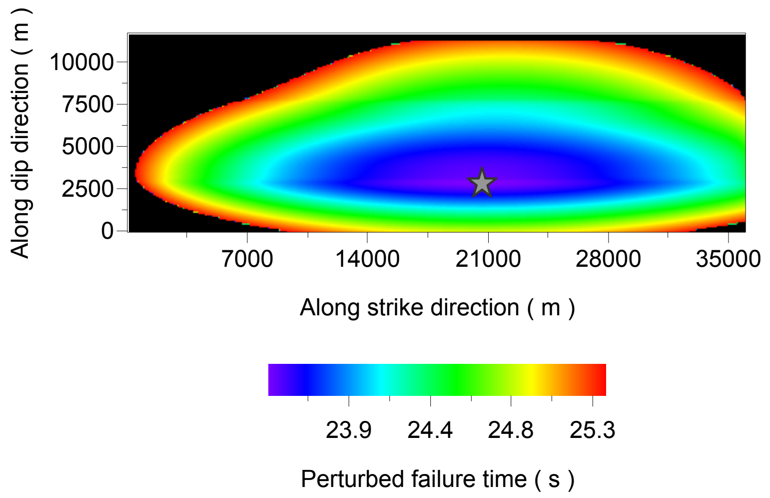


$t_p^{min}$ = 23.47 s @ (20700,2900) m

$M_0$ = 2.37 x $10^{19}$ Nm

Whole fault

*From Bizzarri and Belardinelli (Nov. 2005; subm. to JGR )*

# Results with DR law – homogeneous

## Dieterich – Ruina governing law

$$\tau = \mu(v,\Psi)\,\sigma_n^{eff} = \left[\mu_* + a\,\ln\left(\frac{v}{v_*}\right) + b\,\ln\left(\frac{\Psi\, v_*}{L}\right)\right]\sigma_n^{eff}$$

$$\frac{d}{dt}\Psi = 1 - \frac{\Psi\, v}{L}$$

Can be neglected (see Antonioli et al., 2005)

## Perturbed rupture times

$v(x_1,x_3,t) \geq v_l \;\Rightarrow\; t_p(x_1,x_3) = t$

$v_l$ = 0.1 m/s, in agreement with Belardinelli at al. (2003); Antonioli et al. (2005); Rubin and Ampuero (2005); Ziv and Cochard (2006)

## $\sigma_n^{eff}$ = 2.5 MPa everywhere; acting also $\Delta\sigma_{22}$

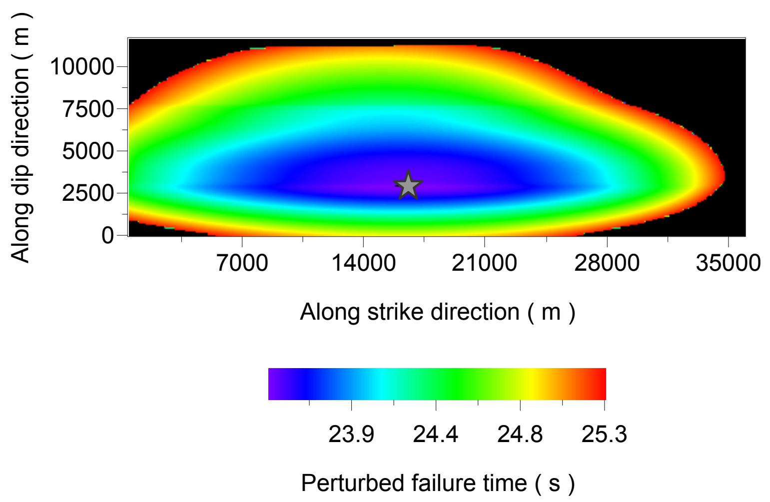


$t_p^{min}$ = 23.47 s @ (16500,2900) m

$M_0$ = 2.23 x $10^{19}$ Nm

Whole fault

*From Bizzarri and Belardinelli (Nov. 2005; subm. to JGR )*

# Results with DR law – heterogeneous

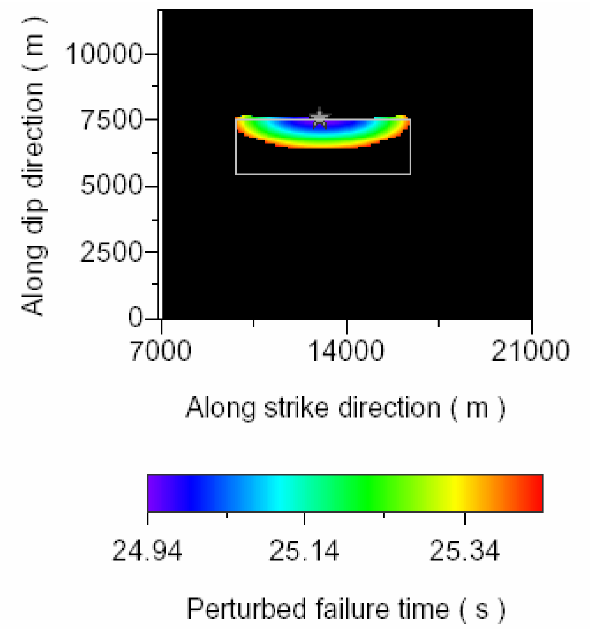


Velocity strengthening behavior ($a > b$) for $x_1 < 9700$ m, $x_1 > 16500$ m, $x_3 > 8800$ m

Effective normal stress profile

$t_p^{min} = 24.94$ s @ (13200,7500) m

$M_0 = 2.27 \times 10^{16}$ Nm

[9700,16500] m in strike direction

[6400,7500] m in dip direction

*From Bizzarri and Belardinelli (Nov. 2005; subm. to JGR )*

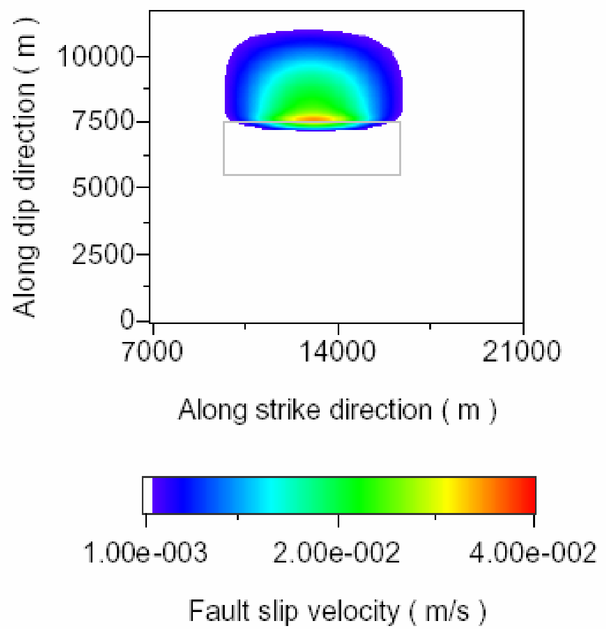


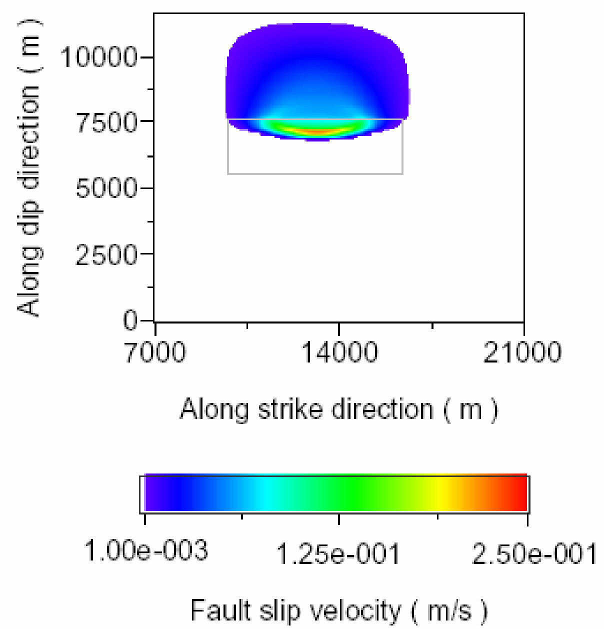


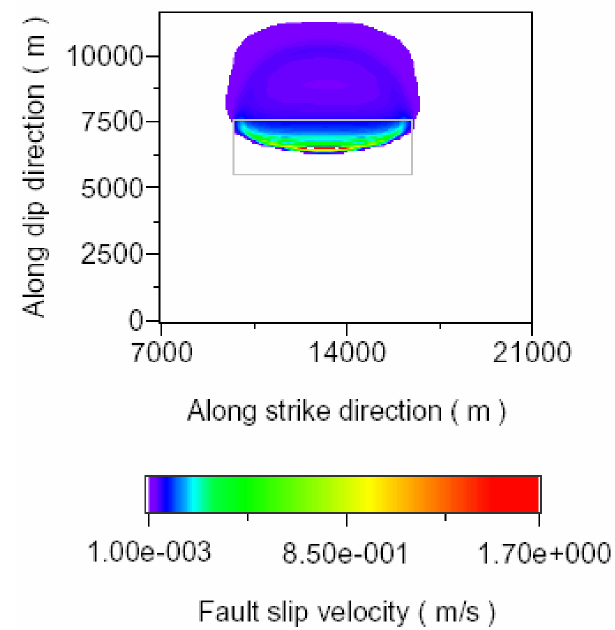

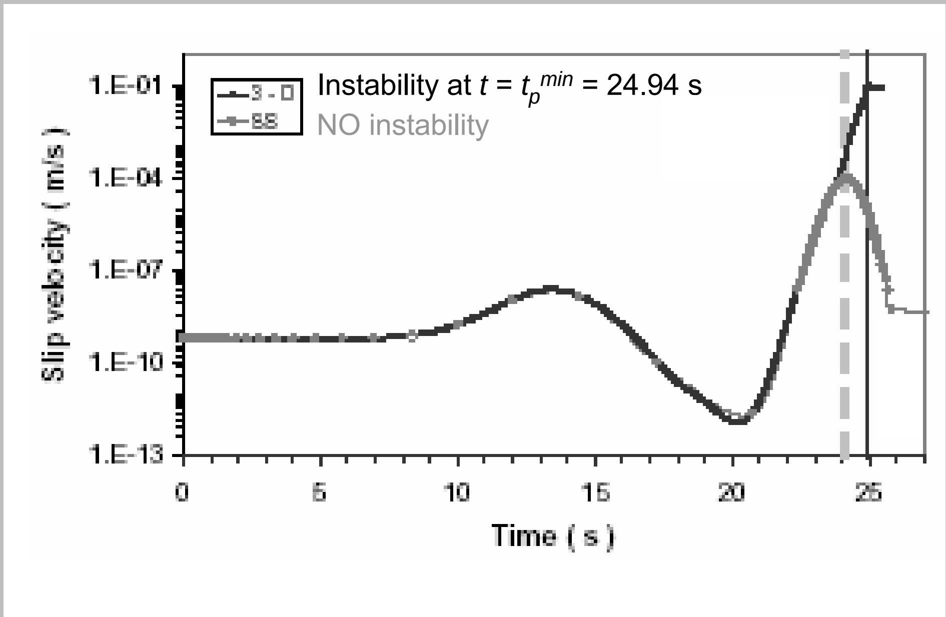


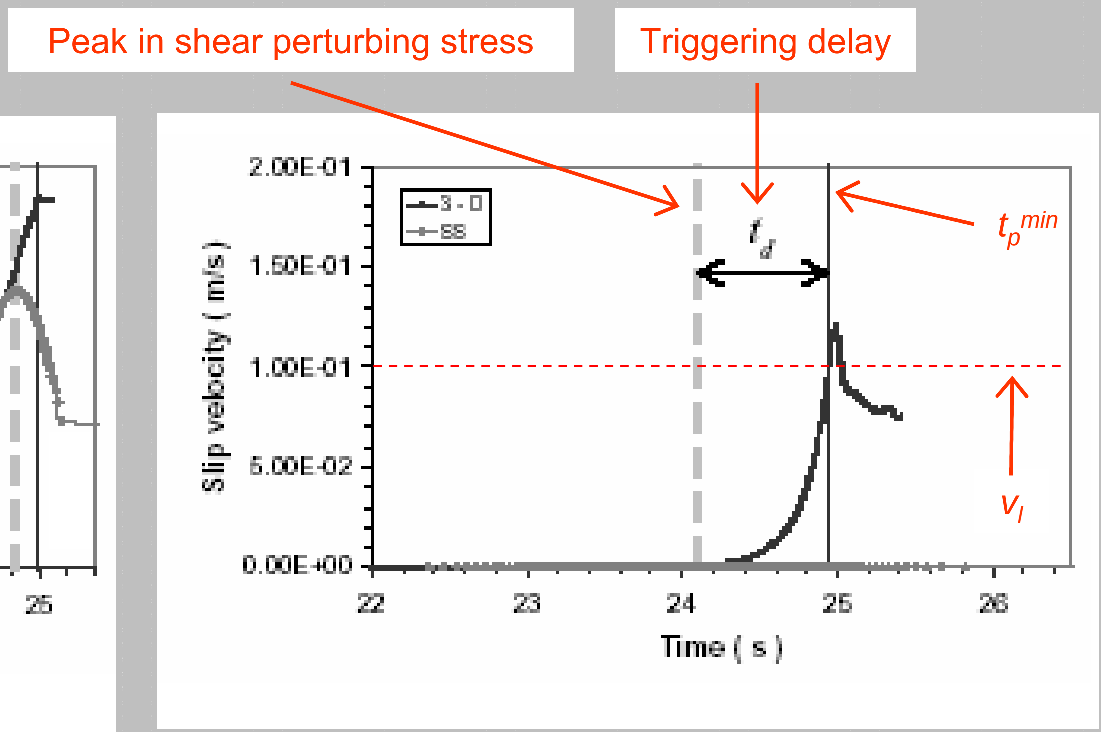


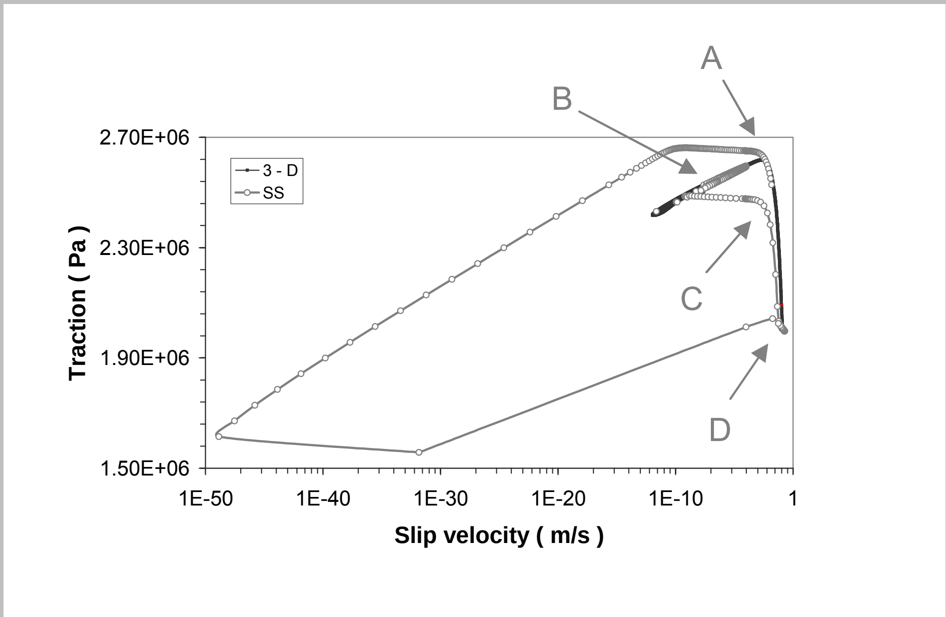


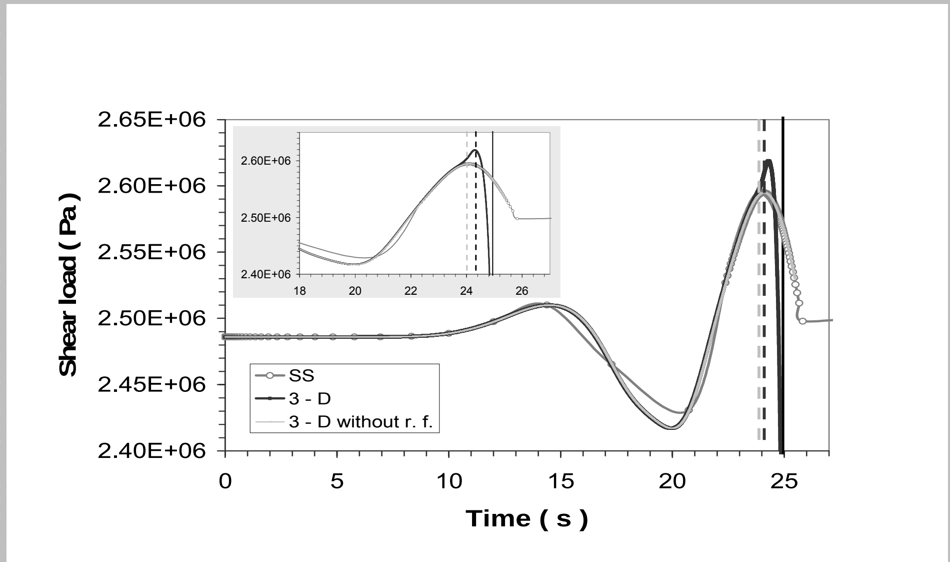


*From Bizzarri and Belardinelli (Nov. 2005; subm. to JGR )*

# Results with RD law – heterogeneous

**Ruina – Dieterich governing law**

$$\tau = \left[ \mu_* + a \ln\left(\frac{v}{v_*}\right) + b \ln\left(\frac{\Psi v_*}{L}\right) \right] \sigma_n^{\,eff}$$

$$\frac{\mathrm{d}}{\mathrm{d}t}\Psi = -\frac{\Psi v}{L} \ln\left(\frac{\Psi v}{L}\right)$$

Can be neglected

$t_p^{min}$ = 23.44 s @ (15700,7900) m

$M_0$ = 2.02 x $10^{16}$ Nm

[9000,17300] m in strike direction

[6300,8000] m in dip direction


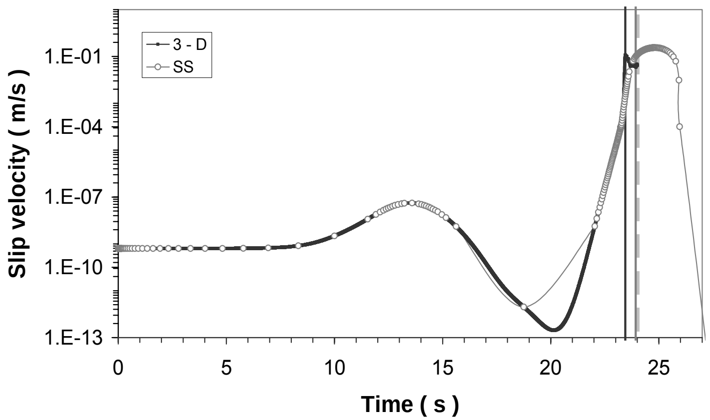


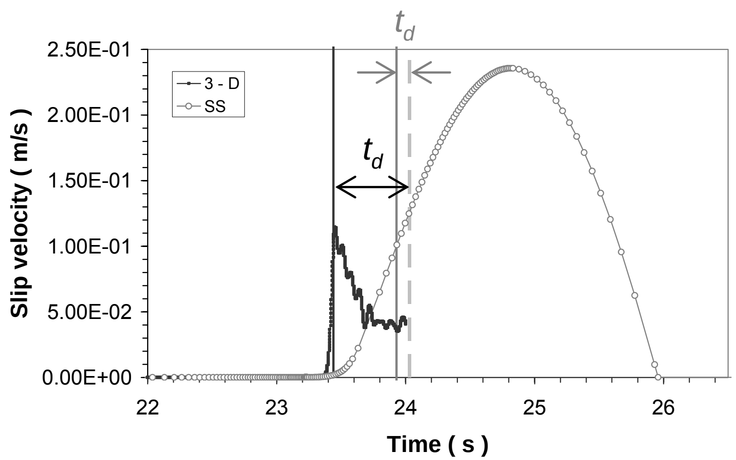


*From Bizzarri and Belardinelli (Nov. 2005; subm. to JGR )*

# In the "virtual" hypocenter

## Dieterich – Ruina governing law

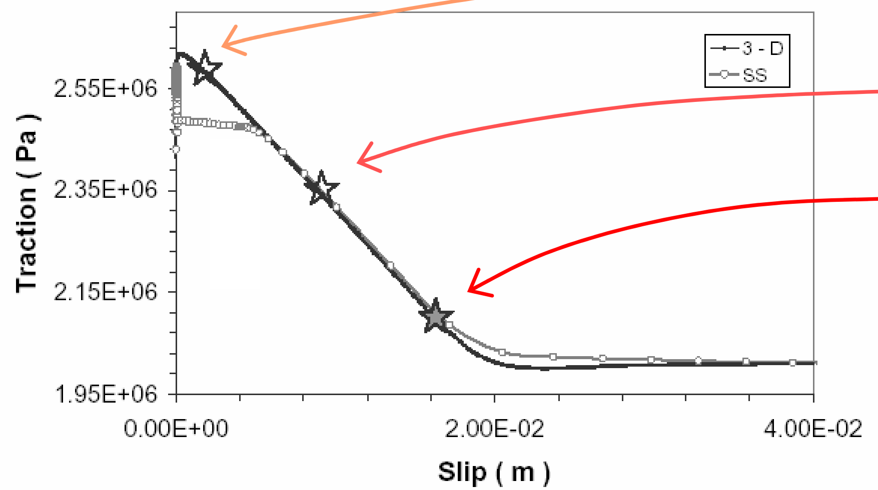


## Ruina – Dieterich governing law

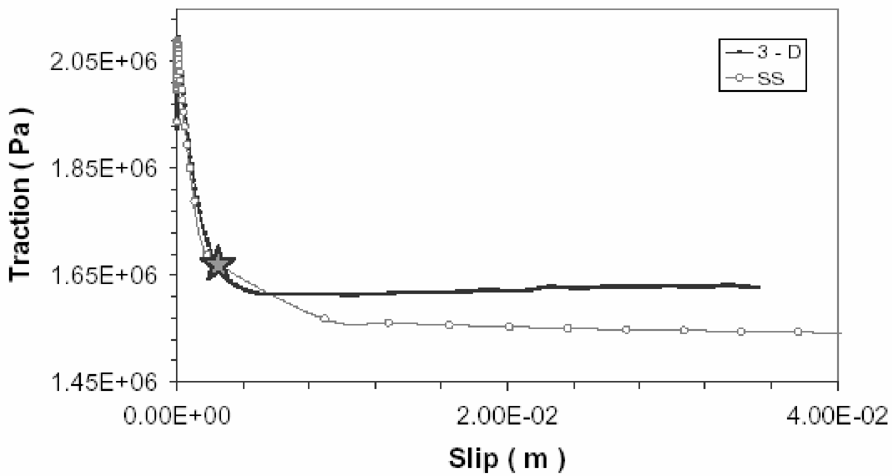


$v^H$ = 0.01 m/s ( $t$ = 24.56 s )

$v^H$ = 0.05 m/s ( $t$ = 24.84 s )

$v^H = v_l$ = 0.1 m/s ( $t = t_p$ = 24.94 s )

Failure occurs before traction reaches the residual level.

RD with $L$ = 5 mm:
$t_p^{min}$ = 23.99 s @ (14600,7600) m
$M_0$ = 1.27 x $10^{16}$ Nm
[9500,16800] m in strike direction
[6500,7700] m in dip direction

RD with $L$ = 10 mm
$t_p^{min}$ = 24.72 s @ (13300,7300) m
$M_0$ = 2.27 x $10^{16}$ Nm
[9500,16700] m in strike direction
[6000,7400] m in dip direction

*From Bizzarri and Belardinelli (Nov. 2005; subm. to JGR )*

# Alternative source time functions

Bouchon source time function:

$$f(t) = \frac{1}{2}\left[1 + \tanh\left(\frac{t}{t_0}\right)\right]$$

Bouchon, 1981; $t_0$ = 1.6 s

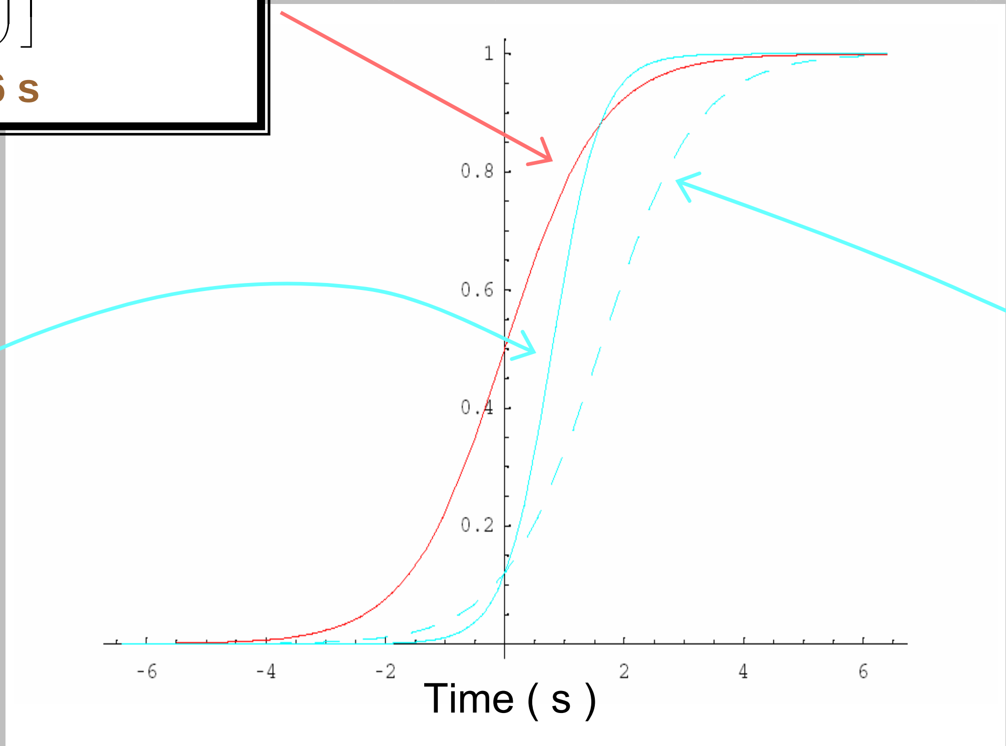


Modified Bouchon source time function:

$$f(t) = \frac{1}{2}\left[1 + \tanh\left(\frac{t - \frac{t_0}{2}}{\frac{t_0}{2}}\right)\right]$$

corrected from Cotton and Campillo, 1995; $t_0$ = 1.6 s

Modified Bouchon source time function:

$$f(t) = \frac{1}{2}\left[1 + \tanh\left(\frac{t - \frac{t_0}{2}}{\frac{t_0}{2}}\right)\right]$$

corrected from Cotton and Campillo, 1995; $t_0$ = 3.2 s

# Alternative source time functions

**Bouchon modificata, $t_0$ = 3.2 s**

$t_p^{min}$ = 26.49 s @ (13000,7500) m

$M_0$ = 2.30 x $10^{16}$ Nm

[9700,16500] m in strike direction

[6400,7600] m in dip direction

**Bouchon modificata, $t_0$ = 1.6 s; $\sigma_n^{eff*}$ = 4.2 MPa**

$t_p^{min}$ = 25.36 s @ (13500,7600) m

$M_0$ = 2.59 x $10^{16}$ Nm

[9500,16700] m in strike direction

[6200,8700] m in dip direction

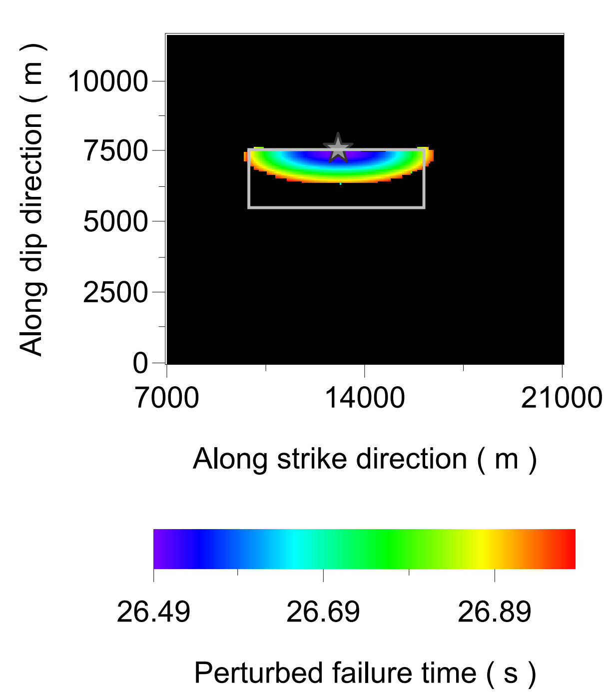


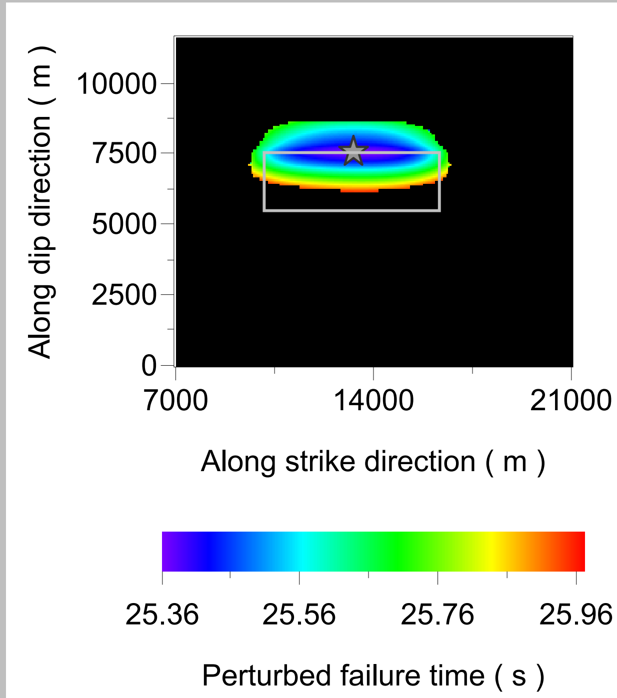


*From Bizzarri and Belardinelli (Nov. 2005; subm. to JGR )*

# Conclusions II

- ✓ We simulate the remote triggering in a truly 3–D fault model with different governing laws;
- ✓ We generalize the results of Antonioli et al. (2006), providing additional details of the 26 s event: the location of the hypocenter, its failure time, the rupture area and the seismic moment;
- ✓ The spring–slider and the 3–D model are intrinsically different, but we observe an excellent agreement during the slow nucleation phase…
- ✓ … during the acceleration, in the 3–D model the dynamic load of the slipping points further decrease the perturbed failure time;
- ✓ Dieterich–Ruina and Ruina–Dieterich laws are valid candidate to model the activation of the Hvalhnúkur fault at 26 s;

- On the contrary, with slip–dependent friction laws it is not possible to simulate the activation of the 26 s aftershock;
- The agreement with observations increases considering a modified (and more causal) source time function;
- If a detailed information of the initial state of the fault, potentially highly heterogeneous, was available the agreement with observations will be even better.

# Synopsis

| *Case* | $\sigma_{n0}^{eff}$ *profile* | *Constitutive law* | *Heterogeneous rheology* | *Rupture extension along strike* (m) | *Rupture extension along dip* (m) | *Hypocenter location* (m) | *Origin time* (s) | *Total seismic moment* $M_0$ (Nm) |
|---|---|---|---|---|---|---|---|---|
| A | (b) | DR | No | Whole fault | Whole fault | (20700,2900) | 23.47 | $2.37 \times 10^{19}$ |
| B | (b) | DR | No | Whole fault | Whole fault | (16500,2900) | 23.47 | $2.23 \times 10^{19}$ |
| C | 1 | DR | No | [0, 27400] | [6000, 11600] | (15400,6600) | 24.08 | $1.94 \times 10^{17}$ |
| D | 2 | DR | No | Not defined | | | | $1.21 \times 10^{14}$ |
| E | 3 | DR | No | [6600, 20000] | [6400, 7500] | (13200,7500) | 24.94 | $6.43 \times 10^{16}$ |
| F | 3 | DR | Yes | [9700, 16500] | [6400, 7500] | (13200,7500) | 24.94 | $2.27 \times 10^{16}$ |
| G | 3 | DR | No | [15700, 35100] | [6000, 7800] | (27300,7500) | 23.44 | $1.22 \times 10^{17}$ |
| H | 3 | RD | Yes | [9000, 17300] | [6300, 8000] | (15700,7900) | 23.44 | $2.02 \times 10^{16}$ |
| I | 3 | RD ($L = 5$ mm) | Yes | [9500, 16800] | [6500, 7700] | (14600,7600) | 23.99 | $1.27 \times 10^{16}$ |
| L | 3 | RD ($L = 10$ mm) | Yes | [9500, 16700] | [6000, 7400] | (13300,7300) | 24.72 | $2.17 \times 10^{16}$ |
| M | 3 | OY | Yes | Not defined | | | | $1.46 \times 10^{14}$ |
| N | 3 | OY | No | Whole fault | Whole fault | (24000,7700) | 23.75 | $2.49 \times 10^{19}$ |
| O | 3 | DR | Yes | [9700, 16500] | [6400, 7600] | (13000,7500) | 26.49 | $2.30 \times 10^{16}$ |
| P | 3 | DR | Yes | [9500, 16700] | [6200, 8700] | (13500,7600) | 25.36 | $2.59 \times 10^{16}$ |
| ***Observational constraints*** | | | | **[9700, 16500]** | **[5400, 7400]** | **($16500 \pm 450$, $8900 \pm 1300$)** | **$25.9 \pm 0.1$** | $\cong$ **$3.2 \times 10^{16}$** |

**This slide is empty intentionally.**

A B R

# Support Slides:
# Parameters, Notes, etc.

*To not be displayed directly. Referenced above.*

# Geothermal areas in Iceland

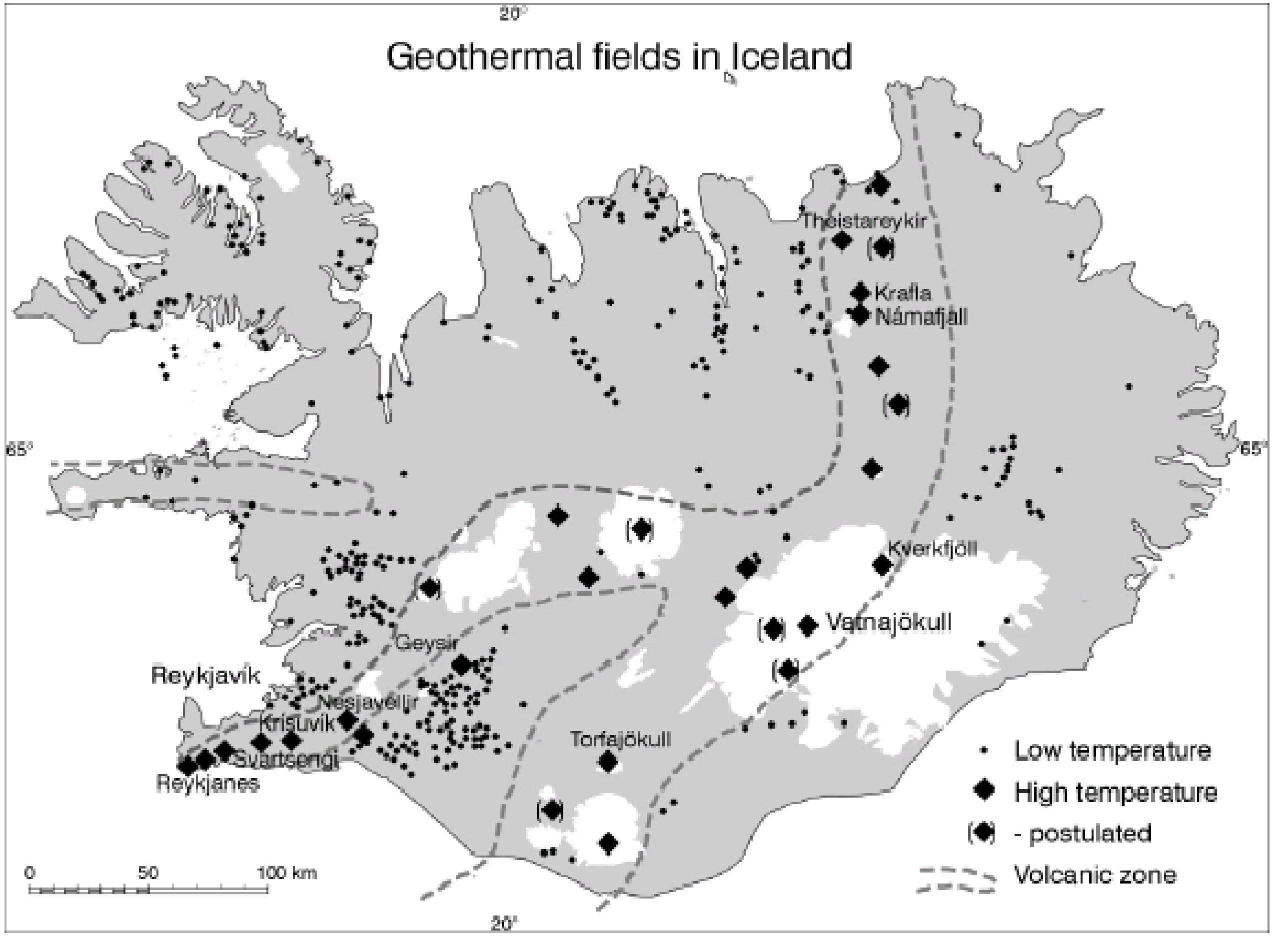


*Proceedings World Geothermal Congress 2000*
*Kyushu - Tohoku, Japan, May 28 - June 10, 2000*

**NATURAL CHANGES IN UNEXPLOITED HIGH-TEMPERATURE GEOTHERMAL AREAS IN ICELAND**

Halldór Ármannsson[1], Hrefna Kristmannsdóttir[1], Helgi Torfason[2] and Magnús Ólafsson[1]
Orkustofnun, [1]Research Division, Geochemistry Department, [2]Energy Management Division
Grensásvegur 9, 108 Reykjavík

Figure 1. Geothermal areas in Iceland. The five main exploited high-temperature areas, Svartsengi, Reykjanes, Nesjavellir, Krafla and Námafjall are shown as well as the four unexploited high-temperature geothermal areas selected for study of natural changes, Krýsuvík, Theistareykir, Torfajökull and Kverkfjöll areas.

| *Parameter* | *Value* |
|---|---|
| $\mathcal{D}$ | parallelepiped that extends $x_{1_{end}} = 36.5$ Km along $x_1$, $x_{2_{end}} = 10$ Km along $x_2$ and $x_{3_{end}} = 11.6$ Km along $x_3$ |
| $\Sigma = \mathcal{FS}$ | $\{ \mathbf{x} \mid x_2 = x_2^f = 5000 \text{ m} \}$ |
| $\Delta x_1 = \Delta x_2 = \Delta x_3 \equiv \Delta x$ | 100 m (a) |
| Number of nodes | 4,289,571 |
| $\Delta t$ | $1.27 \times 10^{-3}$ s (a) |
| Number of time levels | 33,650 |
| $v_l$ | 0.1 m/s |
| $\sigma_n^{eff*}$ | 2.5 MPa |
| $\varphi(x_1, x_3, 0)$ | $\varphi_0 = 180°$ |
| $v(x_1, x_3, 0)$ | $v_{init} = 6.34 \times 10^{-10}$ m/s ( = 20 mm/yr ) |
| $\Psi(x_1, x_3, 0)$ | $\Psi^{ss}(v_{init}) = 1.577 \times 10^{6}$ s ( ≅ 18.25 d ) |
| $\sigma_n^{eff}(x_1, x_3, 0)$ | See Table 3 |
| $\tau_0(x_1, x_3)$ | $\mu^{ss}(v_{init})\sigma_n^{eff}(x_1, x_3, 0)$ |
| $a$ | 0.003 (b) |
| $b$ | 0.010 |
| $L$ | $1 \times 10^{-3}$ m |
| $\mu_*$ | 0.7 |
| $v_*$ | $v_{init}$ |
| $\alpha_{LD}$ | 0 |

Crustal profile (from Vogfjord et al., 2002; Antonioli et al., 2005)

| ***Layer*** # $k$ | $v_{P_k}$ (m/s) | $v_{S_k}$ (m/s) | $\rho_{rock_k}$ (Kg/m$^3$) | ***Up do depth of*** $x_{3_k}$ (m) |
|---|---|---|---|---|
| 1 | 3200 | 1810 | 2300 | 1100 |
| 2 | 4500 | 2540 | 2540 | 3100 |
| 3 | 6220 | 3520 | 3050 | 7800 |
| 4 | 6750 | 3800 | 3100 | 11600 |

# Initial effective normal stress

$$\sigma_{n_0}^{eff}(x_3) \equiv \sigma_n^{eff}(x_1,x_3,t) =$$

$$\begin{cases} \hat{p}^{(litho)}(x_3) - \Delta\sigma^{(dev)} - p_{fluid}^{(hydro)}(x_3) & , x_3 \le x_3^* = 5800\ \text{m} \\ \hat{p}^{(litho)}(x_3) - \Delta\sigma^{(dev)} - \left[ \hat{p}^{(litho)}(x_3) - \Delta\sigma^{(dev)} - \sigma_n^{eff^*} - \Delta P_2\, e^{-\frac{x_3 - x_3^*}{h^*}} + \sigma_n^{eff^*} e^{-\frac{x_3 - x_3^*}{h^*}} \right] & , x_3^* < x_3 < x_3^* + D^* \\ \sigma_n^{eff^*} = 2.5\ \text{MPa} & , x_3 \ge x_3^* + D^* = 8800\ \text{m} \end{cases}$$

$$\Delta P_2 \equiv \hat{p}^{(litho)}(x_3^*) - \Delta\sigma^{(dev)} - p_{fluid}^{(hydro)}(x_3^*)$$